FINAL REPORT

CONTRACT NO. NAS8-28083

"Study on the Effect of Contamination on the Performance of X-Ray Telescopes"

William R. Neal

William P. Reidy

Visidyne, Inc.
19 Third Avenue
Northwest Industrial Park
Burlington, Massachusetts 01803

Prepared for:

George C. Marshall Space Flight Center
Marshall Space Flight Center, Alabama 35813

24 September 1973

FINAL REPORT

CONTRACT NO. NAS8-28083

"Study on the Effect of Contamination on the Performance of X-Ray Telescopes"

William R. Neal

William P. Reidy

Visidyne, Inc.
19 Third Avenue
Northwest Industrial Park
Burlington, Massachusetts 01803

Prepared for:

George C. Marshall Space Flight Center
Marshall Space Flight Center, Alabama 35813

24 September 1973

TABLE OF CONTENTS

FOREWORD

This is the final report on Contract NAS8-28083. This work was in support of a program at the Space Sciences Laboratory, Marshall Space Flight Center, to study the effects of contamination on the performance of x-ray telescopes.

The work performed under this contract was in two general areas. The first area was the modification of the x-ray reflectometer facility to improve its performance and to automate data taking. This effort is discussed in Section 1 of this report. The second area of effort was a program to study the effect of contamination on x-ray telescope performance. This work is discussed in Section 2 and Appendix A of this report.

1. Modification of X-Ray Reflectometer

1.1 Introduction

Two modifications were made to the x-ray reflectometer located at the Space Sciences Laboratory, Marshall Space Flight Center. One was an automatic drive for the Large Micrometer Head. This system, interfaced with the Hewlett Packard Computer System, is used to record data and provides the x-ray reflectometer with an automated data-taking capability. Using this system, a complete scatter curve can be obtained automatically. Previously, it was necessary to manually reset the system after recording for each data point in the scatter curve. The second modification provided an externally controlled electrical drive to move the microfocus x-ray source along its axis. With this modification, one can translate the x-ray source while it is operating to locate the position providing maximum count rate.

1.2 Automatic Drive of the Large Micrometer Head

As originally designed, the x-ray reflectometer sample detector and slit and detector assembly were positioned by a mechanical drive operated through a magnetically coupled vacuum feed through. After each measurement, the micrometer had to be manually positioned for the next measurement. With this modification, the micrometer is automatically advanced between measurements.

Figure 1 is a sketch of the mechanical assembly. The motor, a vacuum rated stepping motor, drives the micrometer head through a six (6) to one (1) gear reduction. The motor advances 1.8 degrees per step. One rotation of the Large Micrometer Head corresponds to an advance of 25 mils. With the 6 to 1 gear reduction 1,200 steps correspond to one rotation of the Large Micrometer Head. Six steps correspond to an advance of .125 mils or 1/8 mil. The unit consists of three assemblies, the large micrometer drive; the control panel; and the preset indicator. The wiring

MICROMETER DRIVE

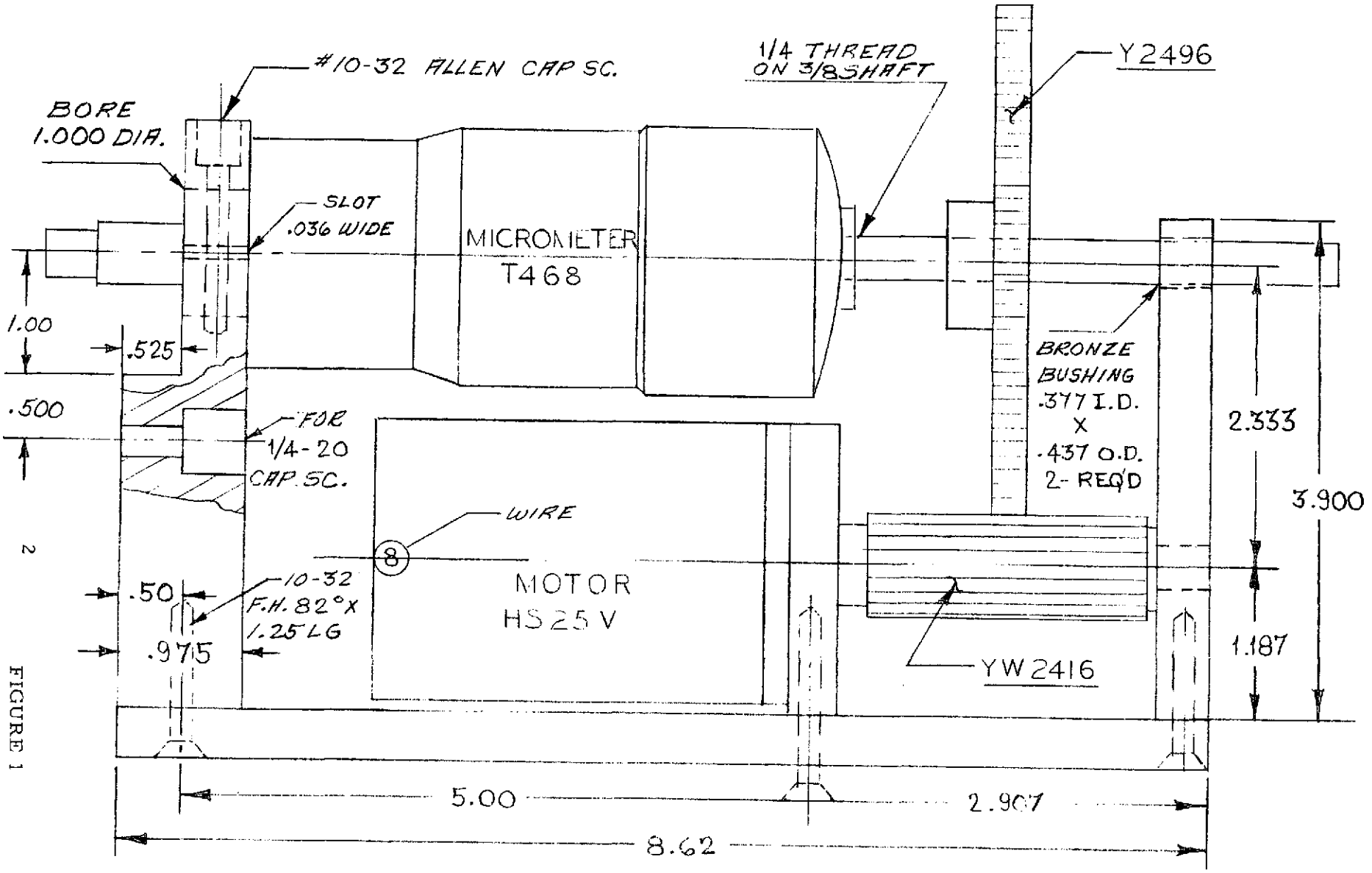

FIGURE 1

schematic is shown in Figure 2. The number of steps per index is set by selection at the front panel of the preset indicator. In the manual mode (control panel switch in Disable) the unit can be run directly from the front panel of the preset indicator. Three control functions are available: Run (continuous stepping); Jog (advance one step); and Index (advance the number of steps selected on the front face of the preset indicator). In either the manual or automatic mode, the direction of motion (forward or reverse) is determined by the position of the Forward/Reverse switch on the control panel.

In the automatic mode, the unit will advance during the computer print out operation the number of steps set on the front panel of the preset indicator. After completion of the predetermined number of steps, the control unit will be disabled for a period of time determined by the setting of the time delay relay in the control panel.

This time should be selected so that the control unit is not enabled (after an advance) until the printing operation is completed. In the automatic mode, the unit will automatically advance during each print out until the micrometer head reaches the limit of travel in one or the other direction. Alternately, the advance can be limited by stopping the computer after a selected number of measurements. The following paragraphs list the instructions for installation, operation, and a listing of the major parts.

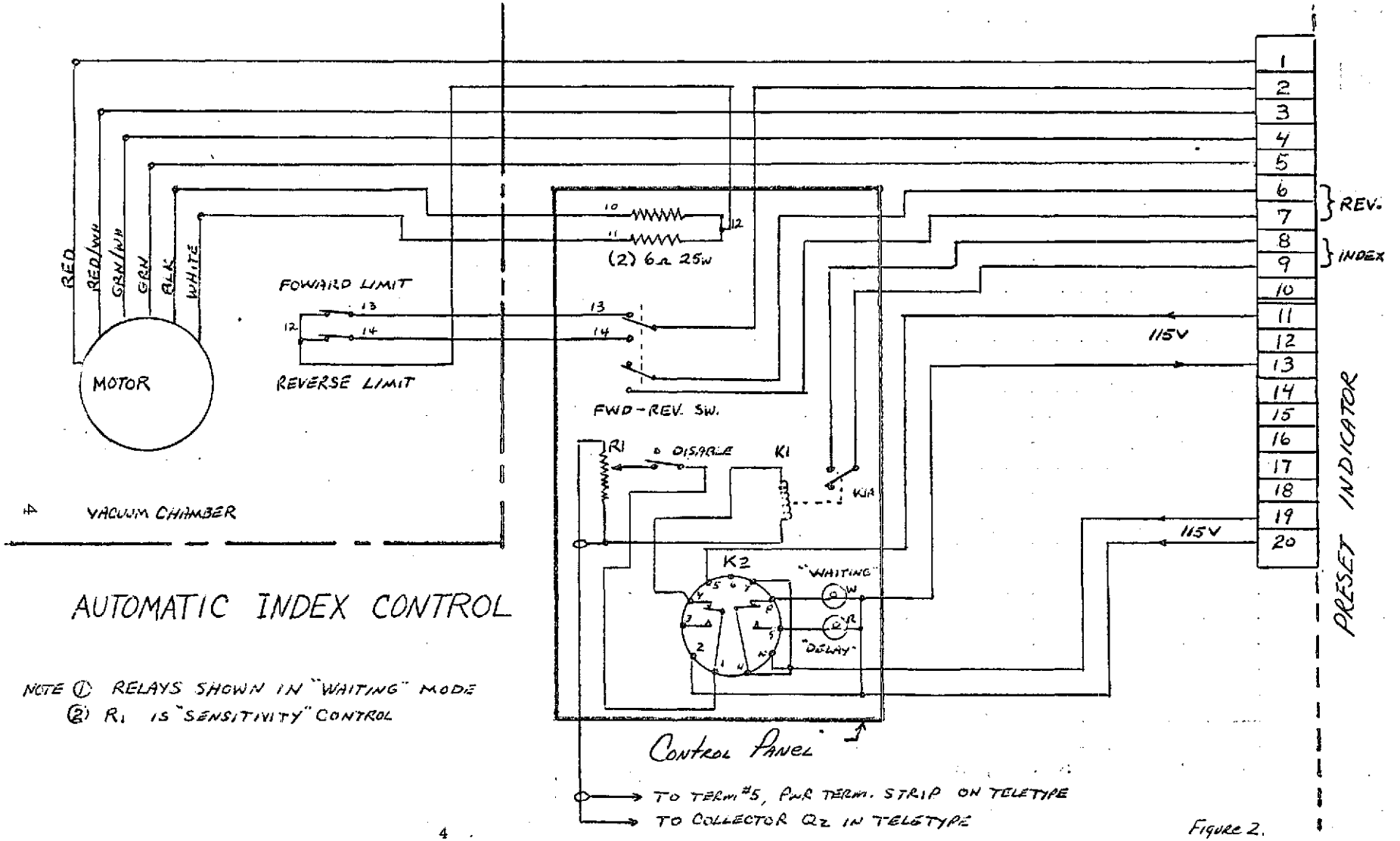

Figure 2.

FIGURE 2

INSTALLATION PROCEDURE

I. Connect all cable leads to indexer unit.
(wire markers indicate terminal strip number)

II. Connect all cable leads to motor feed-thru on vacuum chamber, connect motor.

III. Connect shielded lead to teletype:

a. Center lead connects to lug on collector of QZ (power transistor).

Top cover of the teletype must be removed for this connection.

b. Shield of this lead connects to terminal #5 of power terminal strip on rear lower left of teletype.

IV. Recheck all connections.

V. Turn teletype switch to "Local" position.

VI. Turn on indexer unit and set controls to read 100 on dials. (Red "Delay" light on operators station should come on and after $\approx$ 20 second delay the red light goes out and the white "Waiting" light comes on.

VII. With teletype in Local position and inactive, adjust R, (100K sensitivity adjustment) until the red delay light lights, and motor indexes. Back off on R, approximately 3/4 turn. Wait for red delay light to go out and white waiting light to come on.

VIII. System is now ready to test. Depress any key on teletype, motor will advance, red delay light will light. After motor indexes through whatever number of steps you have selected on front panel, "Delay" then starts and will continue for whatever time you have adjusted on k2.

NOTE: Total time of automatic disable of motor is the combination of time to index plus delay time of k2.

This total time must be at least three (3) seconds longer than the time it takes to type data, otherwise an index pulse will be fed to the motor.

OPERATING INSTRUCTIONS

I. Turn on indexer.

II. Wait for red "Delay" light to go out and white "Waiting" light to come on.

III. Adjust indexer controls to number of steps desired.

IV. Place "Disable" switch on operator's station to "Disable".

V. Type in headings and any other pre-data information.

VI. Pre-set detector arm by pressing "Run" button, ("Jog" button for fine control).

VII. When prepared to take/record data, place "Disable" switch to "Enable" position.

VIII. Motor will automatically index when first data point is typed on teletype.

PARTS LIST

1. HS25V Slo-Syn Stepping Motor
2. Preset Indicator, Slo-Syn SP1800-B5
3. Backlash take-up board, Slo-Syn BHM144134-G1
4. Brass Spur Gear, Boston Gear p/n Y2496 (1)
5. Brass Pinion Gear, Boston Gear p/n YW2416 (1)
6. Micro Switch 11SM3-T (2)
7. Bud SC 2131 Box (1)
8. MST 205N Switch (1)
9. 8-140 Terminal Strip (2)
10. Potter Brimfield Relay CDB-38-70012 (1)
11. Sigma Relay 4F 8000S-SIL (1)
12. IDI #1050A1 Lamp (Red) (1)
13. IDI #1050A2 Lamp (White) (1)
14. Arrow & Hart 81-024-GB Switch (1)
15. 18' Belden Cable, 6 cond. #22 (1)
16. 8' Belden Cable, 2 cond. #22 (1)
17. Amphenol MIP Socket #77MIP8 (1)
18. Ohmite Resistors #25-0362B 7.5Ω 25 w (2)
19. Ohmite Resistors #50-0565 100Ω 50 w (1)

1.3 Electrical Drive X-Ray Tube

The x-ray reflectometer was modified to provide an electrical drive to translate the x-ray tube in one direction. Figure 3 and Figure 4 are mechanical sketches of the modified tube mount. The x-ray tube mount was modified to add a vacuum rated electrical motor gear box and limit switches and necessary mounting fixtures. This modification provided the capability of translating the x-ray tube along its axis using a control external to the vacuum system. The x-ray tube can now be positioned while it is at vacuum pressure and operating to maximize the counting rate of the x-ray reflectometer. An electrical schematic of the modification is shown in Figure 5.

MOTOR MOUNT

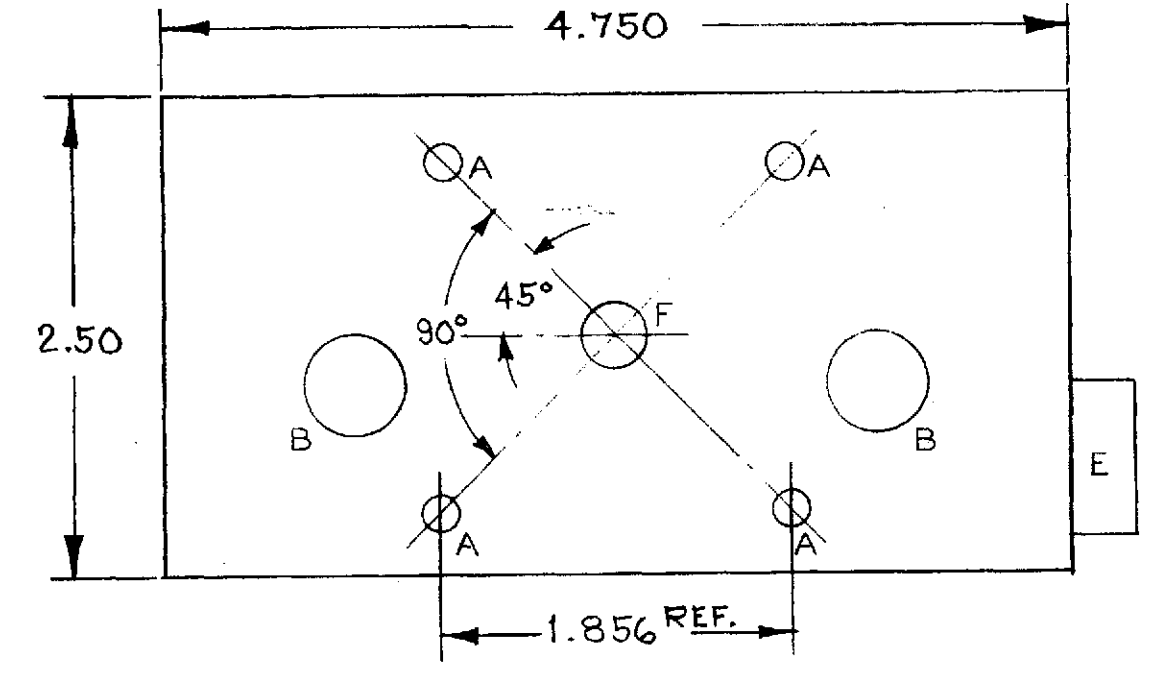

"A" Holes - 10-32 Tap Thru

"B" Holes - .500 Ream Thru

"C" Holes - .187 Pin

"D" Holes - 1/4-20 x .70 DP

"E" - Microswitch BA-2RU22-A2

"F" - .31 Diameter Hole Thru

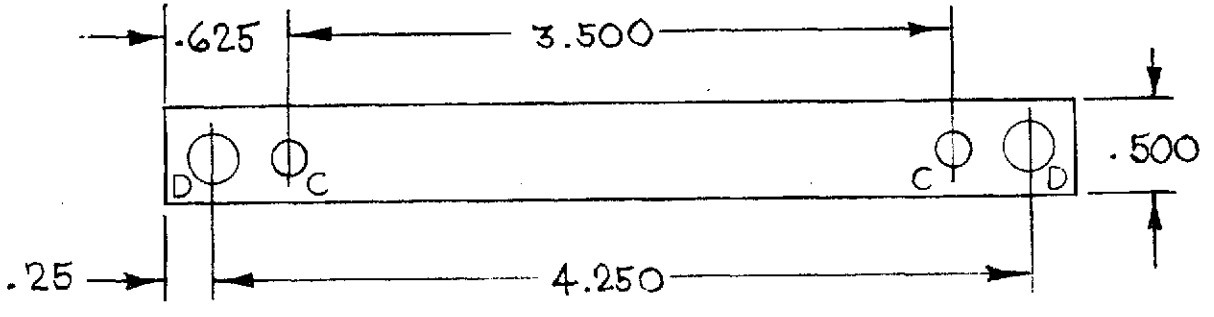

FIGURE 3

MODIFICATION TO X-RAY TUBE HOLDER

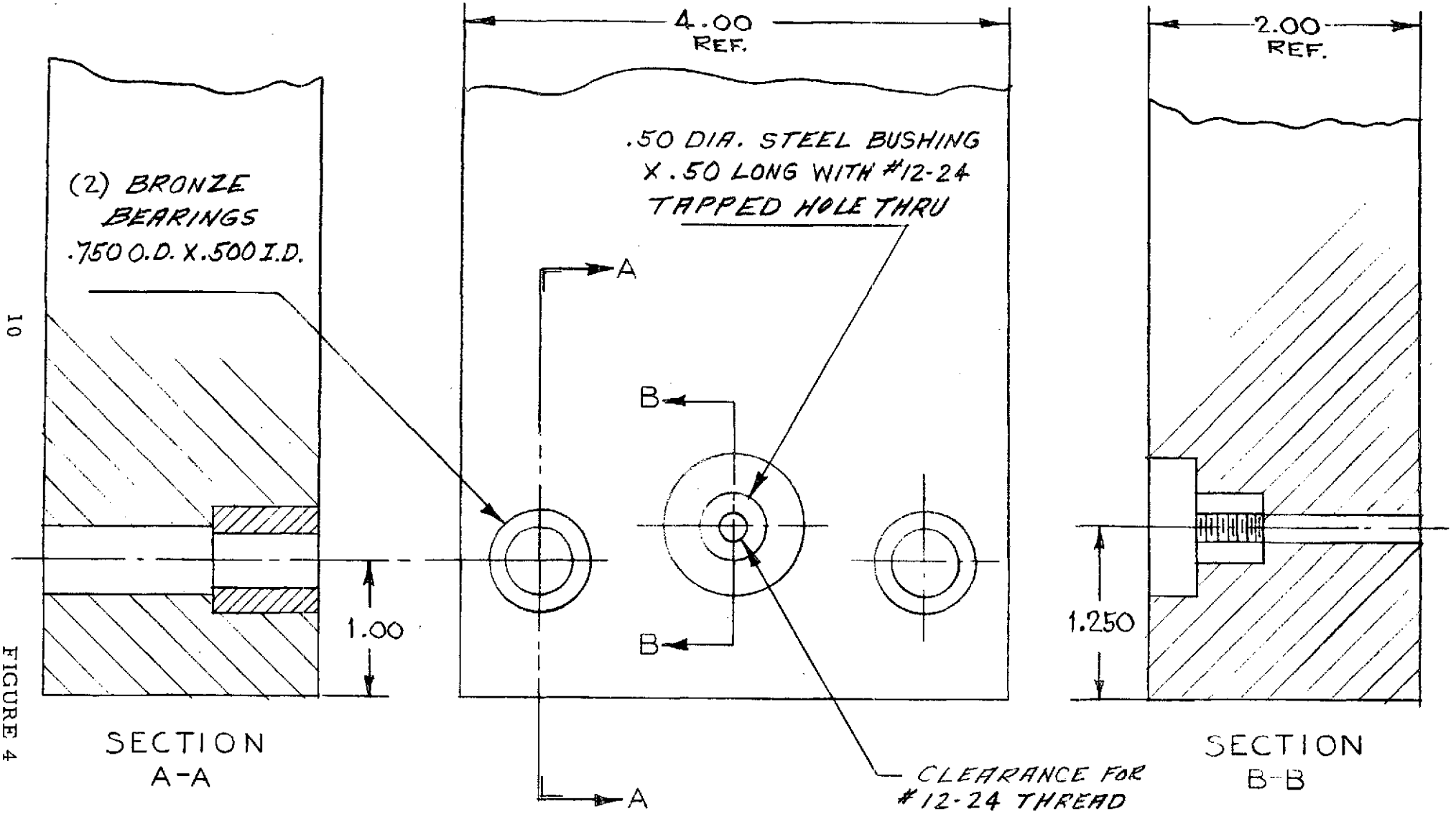

FIGURE 4

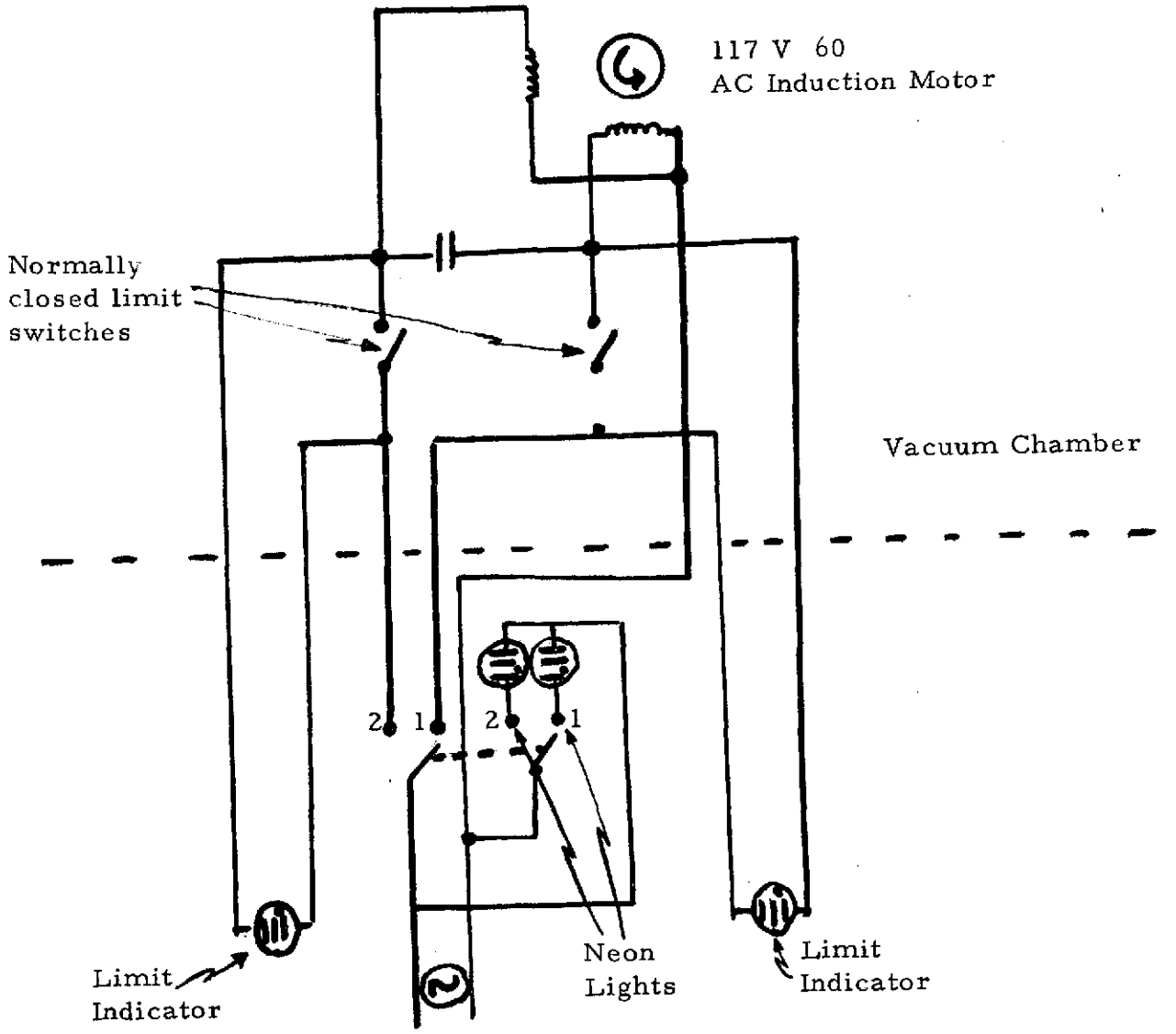
117 V 60
AC Induction Motor
Normally
closed limit
switches
Vacuum Chamber
2
1
2
1
Limit
Indicator
Neon
Lights
Limit
Indicator

FIGURE 5

PARTS LIST

1. SS25V Slo-Syn Synchronous Motor
2. Bushing .75 o.d. x .500 i.d. (4)
3. Thomson External Retaining Rings C-500
4. Stainless Steel Shaft .500 dia. x 10.0" long (2)
5. Micro Switch p/n BA-2RV22-A2 (2)
6. Brass Gears, Boston Gear p/n Y3218 (2)
7. Brass Gears, Boston Gear p/n Y3264 (2)
8. Threaded shaft 12-24
9. Aluminum End Plate (2)

2. Effect of Contamination on the Performance of X-Ray Telescopes

Visidyne has developed a model to calculate the effect of the deposi of foreign materials on polished x-ray reflecting surfaces. Based on this model, a computer program has been developed to calculate reflectivity from polished surfaces and uniform thin films. The program can accomodate either single layers or multiple layers of different densities or materials. The predictions of this model have been compared to previous experimental results.

Appendix A of this document is a technical report on this work.

This page intentionally left blank.

APPENDIX A

TECHNICAL REPORT

"Computer Code for the Calculation of the Glancing X-Ray Reflectivity for a Multilaminate Planar Surface"

This page intentionally left blank.

TECHNICAL REPORT

CONTRACT: NAS 8-28083

Computer Code for the Calculation of the Glancing X-Ray Reflectivity for a Multilaminate Planar Surface

William R. Neal

Visidyne, Inc.
19 Third Avenue
Northwest Industrial Park
Burlington, Massachusetts 01803

Prepared for:

George C. Marshall Space Flight Center
Marshall Space Flight Center, Alabama 35812

12 April 1973

TABLE OF CONTENTS

1.0 INTRODUCTION

Program RFLTBL computes the reflected intensity as a function of the angle of incidence of an x-ray beam incident at grazing angles on a laminated planar surface. This computation is performed in two distinct steps.

Subroutines FDELTA and FBETA calculate the real and imaginary components, δ and β, of the complex index of refraction from the more readily accessible physical parameters such as density, x-ray absorption coefficients and their wavelength dependence, atomic level oscillator strengths, and the like. Subroutine XREFL, given the thickness and complex index of refraction for each layer of an array, calculates the reflectance at a given angle of incidence. The main program, RFLTBL, reads in the relevant layer data, layer by layer, and prints it out as part of the output; calls FDELTA and FBETA into play to compute the required indices of refraction, and prints them out in tabular form; using XREFL, generates a stored table of reflectance values vs. angles of incidence and prints that out; and, if requested, passes the stored tables to a plotting program for direct graphical output. The program is a circulating one so that any number of cases (i.e., a reflectance vs. angle table for a given set of layer data) may be processed in a single job.

2.0 THEORY AND APPROACH

There are two major areas of computation to be considered — (a) calculating the reflected intensity from a planar laminated surface— given the necessary complex indices of refraction and layer depths — and (b) calculating the indices of refraction from more basic data.

2.1 X-Ray Reflection from Multi-layer Surfaces

2.1.1 Electromagnetic Plane Wave in a Dissipative Medium

If the charge density ρ is zero in a medium, and the current density is given by

$$j = \sigma \vec{E}$$

then Maxwell's equations become[1]

$$\nabla \cdot \vec{E} = 0$$

$$\nabla \times \vec{E} = -\mu \frac{\partial \vec{H}}{\partial t} \simeq -\mu_o \frac{\partial \vec{H}}{\partial t}$$

$$\nabla \cdot \vec{H} = 0$$

$$\nabla \times \vec{H} = \sigma \vec{E} + \epsilon_{rel.} \epsilon_o \frac{\partial \vec{E}}{\partial t}$$

In terms of the MKS free-space electric permittivity and magnetic permeability, ϵ_o and μ_o, one defines the free-space speed of light

$$c = \frac{1}{\sqrt{\epsilon_o \mu_o}}$$

and the electromagnetic field impedance

$$\eta_o = \sqrt{\frac{\mu_o}{\epsilon_o}}$$

Since only steady-state, monochromatic solutions are required, complex number methods greatly facilitate analysis and accordingly one defines

$$\vec{E}(\vec{r}, t) = \hat{\vec{E}}(\vec{r})\, e^{i\omega t}$$

and

$$\vec{H}(\vec{r}, t) = \hat{\vec{H}}(\vec{r})\, e^{i\omega t}$$

where $\hat{E}$ and $\hat{H}$ are the complex (indicated by the superposed circumflex) spatial amplitudes.

In terms of these definitions, the non-zero Maxwell equations become

$$\nabla \times \hat{\vec{E}} = -i \frac{\omega}{c} (\eta_o H)$$

and

$$\nabla \times (\eta_o \hat{\vec{H}}) = i \frac{\omega}{c} \left(\epsilon_{rel.} - i \frac{\eta_o c \sigma}{\omega} \right) \hat{\vec{E}}$$

showing that use of a complex dielectric constant

$$\hat{\epsilon} = \epsilon_R - i \epsilon_I$$

$$\equiv \epsilon_{rel.} - i \frac{\eta_o c \sigma}{\omega}$$

i.e., where

$$\epsilon_R = \epsilon_{rel.}$$

and

$$\epsilon_I = \frac{\eta_o c \sigma}{\omega}$$

(and no explicit conduction current)is equivalent to treating a dissipative medium with a purely real dielectric constant.

Plane-wave solutions of the type

$$\vec{E}(\vec{r},t) = \hat{\vec{E}}_\omega \, e^{i(\omega t - \vec{k}\cdot\vec{r})}$$

and

$$\vec{H}(\vec{r},t) = \hat{\vec{H}}_\omega \, e^{i(\omega t - \vec{k}\cdot\vec{r})}$$

can exist if the wave-vector $\vec{k}$ satisfies

$$\vec{k} \times \hat{\vec{E}}_\omega = \frac{\omega}{c} (\mathcal{Z}_o \hat{\vec{H}}_\omega)$$

and

$$\vec{k} \times (\mathcal{Z}_o \hat{\vec{H}}_\omega) = \frac{-\omega}{c} \hat{\epsilon} \hat{\vec{E}}_\omega$$

Inserting the first equation (for $\mathcal{Z}_o \hat{\vec{H}}_\omega$) into the second yields a condition on $\vec{k}$:

$$\vec{k}^2 = (\frac{\omega}{c})^2 \hat{\epsilon} = (\frac{\omega}{c})^2 (\epsilon_R - i\,\epsilon_I)$$

so that $\vec{k}$ must be a complex quantity:

$$\hat{\vec{k}} = \vec{k}_R - i\,\vec{k}_I$$

The plane-wave factor for the E- and H- fields then becomes

$$e^{i(\omega t - \hat{\vec{k}}\cdot\vec{r})} = e^{-\vec{k}_I\cdot\vec{r}} \, e^{i(\omega t - \vec{k}_R\cdot\vec{r})}$$

showing explicitly the attenuation brought about by the complex dielectric constant. For a pure transverse electromagnetic wave ($\vec{E}\cdot\vec{H} = 0$, $\vec{k}_R\cdot\vec{E} = 0 = \vec{k}_R\cdot\vec{H}$) the directions of propagation and attenuation are the same, so that

$$\begin{aligned} \hat{k}^2 &= (\vec{k}_R - i\,\vec{k}_I)\cdot(\vec{k}_R - i\,\vec{k}_I) \\ &= k_R^2 - k_I^2 - 2\,i\,k_R\,k_I \\ &= (\frac{\omega}{c})^2 (\epsilon_R - i\,\epsilon_I) \end{aligned}$$

which can be solved for

$$k_R = \frac{\omega}{c} \sqrt{\frac{1}{2} \left[\sqrt{\epsilon_R^2 + \epsilon_I^2} + \epsilon_R \right]}$$

and

$$k_I = \frac{\omega}{c} \sqrt{\frac{1}{2} \left[\sqrt{\epsilon_R^2 + \epsilon_I^2} - \epsilon_R \right]}$$

In what follows it proves convenient to introduce two defined quantities:

$$\hat{\vec{\mathcal{H}}} \equiv \beta_o \hat{\vec{H}}$$

and

$$\hat{\vec{\kappa}} \equiv \hat{\vec{k}} / (\omega/c)$$

such that

$$\hat{\vec{\kappa}}^2 = \left(\frac{c}{\omega}\right)^2 \hat{\vec{k}}^2 = \hat{\epsilon} = \epsilon_R - i\,\epsilon_I$$

$$= \hat{n}^2$$

where $\hat{n}$ ($= \sqrt{\hat{\epsilon}}$) is the complex index of refraction of the medium. Also, the non-zero Maxwell equations become

$$\hat{\vec{\kappa}} \times \hat{\vec{E}} = \hat{\vec{\mathcal{H}}}$$

and

$$\hat{\vec{\kappa}} \times \hat{\vec{\mathcal{H}}} = -\hat{\epsilon}\,\hat{\vec{E}}$$

2.1.2 Electromagnetic Plane Waves in a Multi-layer Medium

When an electromagnetic plane wave is obliquely incident on a multi-layered medium, the steady-state result is characterized by the presence in each layer of two plane waves[2] — an advancing "transmitted" wave, and a returning "reflected" wave. These are, in turn, characterized by complex amplitudes and wave-vectors, $\hat{\vec{E}}^{\pm}$ and $\hat{\vec{k}}^{\pm}$, where the + and - serve to distinguish transmitted and reflected values. At each interface of two media, continuity of tangential components of the $\vec{E}$ and $\vec{H}$ fields along the interface gives rise to relationships between the field amplitudes and wave-vector components of the two media. Since each layer is treated formally in the same manner, a matric approach will prove most convenient.

In the diagram below

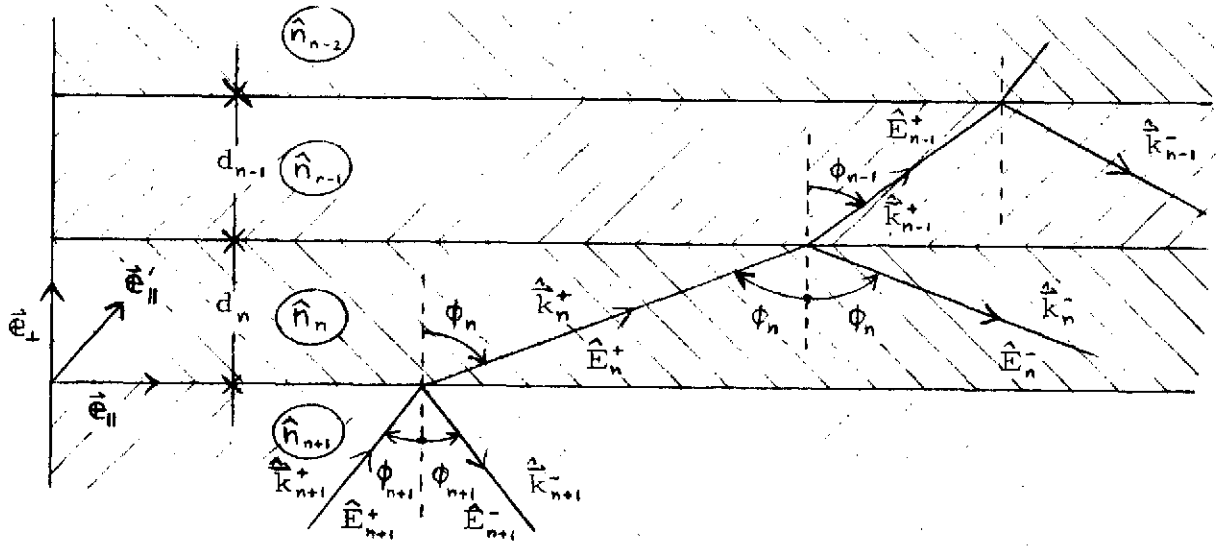

the pertinent variables associated with a typical n^{th} layer are schematically indicated, where d_n is the layer thickness, $\hat{n}_n$ ($= \sqrt{\epsilon_n}$) is the complex index of refraction of the medium,

and ϕ_n is the angle (relative to the interface normal) of the wave-vectors, $\hat{\vec{k}}_n^{\pm}$. The unit base vector triad is defined as follows. The vector $\vec{e}_\perp$ is the interface normal, pointing in the direction of the transmitted wave. The vector $\vec{e}_{\parallel}$ is a vector that is parallel to the interface and lies in the plane of incidence as defined by $\vec{e}_\perp$ and $\hat{k}^+$. The other vector parallel to the interface is defined as $\vec{e}_{\parallel}' = \vec{e}_\perp \times \vec{e}_{\parallel}$.

The two waves in the n^{th} medium have the form

$$\hat{\vec{E}}_n^{\pm}(\vec{r}, t) = \hat{\vec{E}}_n^{\pm} e^{i(\omega t - \hat{\vec{k}}_n^{\pm} \cdot \vec{r})} = \hat{\vec{E}}_n^{\pm} e^{i\frac{\omega}{c}(ct - \hat{\vec{\varkappa}}_n^{\pm} \cdot \vec{r})}$$

where

$$\hat{\vec{\varkappa}}_n^{\,2} = \left(\frac{c}{\omega}\right)^2 \hat{\vec{k}}_n^{\,2} = \hat{n}_n^{\,2} = \hat{\epsilon}_n$$

The components of $\varkappa_n^{\pm}$ normal and parallel to the interface are

$$\hat{\varkappa}_{n_\perp}^{\pm} = \hat{\vec{\varkappa}}_n^{\pm} \cdot \vec{e}_\perp = \pm \hat{n}_n \cos\phi_n$$

and

$$\hat{\varkappa}_{n_{\parallel}}^{\pm} = \hat{\vec{\varkappa}}_n^{\pm} \cdot \vec{e}_{\parallel} = \hat{n}_n \sin\phi_n$$

For the tangential components to be continuous at all points on the interface, and for all times, the generalized Snell's Law must prevail:

$$n_{inc} \sin\phi_{inc} = \ldots = \hat{n}_n \sin\phi_n = \hat{n}_{n+1} \sin\phi_{n+1} = \ldots$$

where the index of refraction of the incidence medium (usually air or vacuum) is taken as purely real. Since $\hat{n}_n$ is in general

complex, and $\hat{n}_n \sin \phi_n$ (equal to $n_{inc} \sin \phi_{inc}$) is real, $\sin \phi_n$ may be complex:

$$\sin \phi_n = n_{inc} \sin \phi_{inc} / \hat{n}_n$$

in terms of which

$$\hat{n}_n \cos \phi_n = \sqrt{\hat{n}_n^2 - \hat{n}_n^2 \sin^2 \phi_n}$$

$$= \sqrt{\hat{n}_n^2 - n_{inc}^2 \sin^2 \phi_{inc}}$$

which also may be complex.

In the following, two quantities occur frequently enough to warrant definitions[3]:

$$a_{n,n-1} \equiv \frac{\hat{\mathcal{H}}^{\pm}_{n-1\perp}}{\hat{\mathcal{H}}^{\pm}_{n\perp}} = \frac{\hat{n}_{n-1} \cos \phi_{n-1}}{\hat{n}_n \cos \phi_n}$$

(by virtue of the generalized Snell's Law, the corresponding ratio of parallel components is unity, requiring no further definitions)

and the phase difference, ψ_n, between in-line points on opposite interfaces ($\Delta \vec{r}_n = d_n \vec{e}_\perp$)

$$\hat{\psi}_n = \hat{\vec{k}}^+_n \cdot \Delta \vec{r}_n = \frac{\omega}{c} d_n \hat{\mathcal{H}}_n \cdot \vec{e}_\perp$$

$$= \frac{\omega}{c} d_n \hat{n}_n \cos \phi_n$$

To simplify the treatment of tangential field component continuity, it is convenient to consider an arbitrarily polarized plane wave as a linear combination of two plane waves whose electric vector is either parallel (π-case) or perpendicular (σ-case) to the plane of incidence. Continuity considerations then yield for the σ-case:

$$E^{+}_{n+1} = \frac{1}{2}\,(1 + a_{n+1,n})\; e^{i\psi_n}\; E^{+}_{n} + \frac{1}{2}\,(1 - a_{n+1,n})\; e^{-i\psi_n} E^{-}_{n}$$

and

$$E^{-}_{n+1} = \frac{1}{2}\,(1 - a_{n+1,n})\; e^{i\psi_n}\; E^{+}_{n} + \frac{1}{2}\,(1 + a_{n+1,n})\; e^{-i\psi_n} E^{-}_{n}$$

and (in terms of $\mathcal{H} = \zeta_o H$, for reasons of simplicity) for the π-case:

$$\mathcal{H}^{+}_{n+1} = \frac{1}{2}\left[1 + \left(\frac{\hat{n}_{n+1}}{\hat{n}_n}\right)^2 a_{n+1,n}\right] e^{i\psi_n}\,\mathcal{H}^{+}_{n} + \frac{1}{2}\left[1 - \left(\frac{\hat{n}_{n+1}}{\hat{n}_n}\right)^2 a_{n+1,n}\right] e^{-i\psi_n}\,\mathcal{H}^{-}_{n}$$

and

$$\mathcal{H}^{-}_{n+1} = -\frac{1}{2}\left[1 - \left(\frac{\hat{n}_{n+1}}{\hat{n}_n}\right)^2 a_{n+1,n}\right] e^{i\psi_n}\,\mathcal{H}^{+}_{n} - \frac{1}{2}\left[1 - \left(\frac{\hat{n}_{n+1}}{\hat{n}_n}\right)^2 a_{n+1,n}\right] e^{-i\psi_n}\,\mathcal{H}^{-}_{n}$$

These multi-layer results can be expressed in terms of the reflection and transmission coefficients for the interface of two semi-infinite media[3]:

$$r_{n+1,n} = \frac{1 - a_{n+1,n}}{1 + a_{n+1,n}} \qquad (\sigma\text{-case})$$

$$= -\frac{1 - \left(\frac{\hat{n}_{n+1}}{\hat{n}_n}\right)^2 a_{n+1,n}}{1 + \left(\frac{\hat{n}_{n+1}}{\hat{n}_n}\right)^2 a_{n+1,n}} \qquad (\pi\text{-case})$$

$$t_{n+1,n} = \frac{2}{1 + a_{n+1,n}} \qquad (\sigma\text{-case})$$

$$= \frac{2\left(\frac{\hat{n}_{n+1}}{\hat{n}_n}\right)}{1 + \left(\frac{\hat{n}_{n+1}}{\hat{n}_n}\right)^2 a_{n+1,n}} \qquad (\pi\text{-case})$$

If the $\mathcal{H}^{\pm}$ equations are changed to equivalent $E^{\pm}$ equations by the relationship

$$\hat{\mathcal{H}}_n^2 = (\hat{\kappa}_n \times \hat{E}_n)^2 = \hat{\kappa}_n^2 \hat{E}_n^2 - (\hat{\kappa}_n \cdot \hat{E}_n)^2 = \hat{n}_n^2 \hat{E}_n^2$$

then there obtains the simple result [4]

$$\vec{E}_{n+1} = \mathbb{M}_n \vec{E}_n$$

where

$$\vec{E}_n = \begin{pmatrix} E_n^+ \\ E_n^- \end{pmatrix}$$

and

$$\mathbb{M}_n = \frac{1}{t_{n+1,n}} \begin{pmatrix} e^{i\psi_n} & r_{n+1,n} e^{-i\psi_n} \\ r_{n+1,n} e^{i\psi_n} & e^{-i\psi_n} \end{pmatrix}$$

where the appropriate π-case or σ-case $r_{n+1,n}$ and $t_{n+1,n}$ coefficients are to be used.

2.1.3 Reflection Coefficient of Multi-layer Medium

The general geometry of the N-layer (plus substrate) problem consists of one semi-infinite medium (with real index of refraction n_{N+1}) in which both the incident beam is coming from a source at infinity and the reflected beam is returning; a set of N plane parallel layers of finite thickness

(with possibly complex indices $\hat{n}_1$, $\hat{n}_2$, $\ldots . \hat{n}_N$); and another semi-infinite medium, the substrate, (with possibly complex index $\hat{n}_o$) in which the transmitted beam goes to infinity. The phase convention is adopted wherein the field amplitude in the k^{th} medium is defined as that at the interface of the k^{th} and $(k-1)^{th}$ media. The substrate, however, has no true corresponding "-1^{st}" companion interface to its "0^{th}" (medium 1/medium 0) interface and requires special consideration. If the transmitted beam, $E_{trans} = E_o^+$, is desired at a point d_o into the substrate, a conceptual interface through d_o can be considered to separate the substrate into two regions, the "0^{th}" and "-1^{st}", both having the same index of refraction, $\hat{n}_o$, so there is unit transmission. Then, making the identifications

$$E_{N+1}^+ = E_{inc}$$

$$E_{N+1}^- = E_{refl}$$

$$E_o^+ = E_{trans}(do)$$

$$E_o^- \equiv 0$$

and using the previously derived $\mathbb{M}$-matrices:

$$\begin{pmatrix} E_{inc} \\ E_{refl} \end{pmatrix} = \begin{pmatrix} E_{N+1}^+ \\ E_{N+1}^- \end{pmatrix} = \vec{E}_{N+1}$$

$$= \mathbb{M}_N \vec{E}_N$$

$$= \mathbb{M}_N \mathbb{M}_{N-1} \vec{E}_{N-1}$$

$$\vdots$$

$$= \mathbb{M}_N \mathbb{M}_{N-1} \ldots \mathbb{M}_k \vec{E}_k$$

$$\equiv \mathbb{M}_{N,k} \vec{E}_k$$

If there is no total reflection from any interface, then the amplitudes $E_1^{\pm}$ at the medium 1/substrate interface are related to the single substrate amplitude E_o^+ $(d_o = 0+)$ by

$$E_1^- = r_{10}\, E_1^+$$

and

$$E_0^+ = t_{10}\, E_1^+$$

so that

$$\begin{pmatrix} E_{inc} \\ E_{refl} \end{pmatrix} = \mathcal{M}_{N,1}\, \vec{E}_1 = \mathcal{M}_{N,1} \begin{pmatrix} E_1^+ \\ r_{10}\, E_1^+ \end{pmatrix}$$

$$= E_1^+\, \mathcal{M}_{N,1} \begin{pmatrix} 1 \\ r_{10} \end{pmatrix}$$

If the matrix elements of $\mathcal{M}_{N,1}$ are defined as

$$\mathcal{M}_{N,1} = \begin{pmatrix} M_{11} & M_{12} \\ M_{21} & M_{22} \end{pmatrix}$$

then the reflection coefficient, r_N, for the N-layer array is given by

$$r_N = \frac{E_{refl}}{E_{inc}} = \frac{M_{21} + M_{22}\, r_{10}}{M_{11} + M_{12}\, r_{10}}$$

If there is total reflection from the medium k/medium k-1 interface, there results

$$E_k^- = r_{k,k-1}\, E_k^+$$

$$E_{k-1}^{\pm} = 0$$

so that

$$\begin{pmatrix} E_{inc} \\ E_{refl} \end{pmatrix} = \mathbb{M}_{N,k} \vec{E}_k = \mathbb{M}_{N,k} \begin{pmatrix} E_k^+ \\ r_{k,k-1} E_k^+ \end{pmatrix}$$

$$= E_k^+ \mathbb{M}_{N,k} \begin{pmatrix} 1 \\ r_{k,k-1} \end{pmatrix}$$

and

$$r_N = \frac{E_{refl}}{E_{inc}} = \frac{M_{21} + M_{22} r_{k,k-1}}{M_{11} + M_{12} r_{k,k-1}}$$

Thus, in general, the reflectance R of an N-layer surface is given by the squared magnitude of the reflection coefficients, r_N,

$$R = r_N r_N^*$$

where r_N is determined from the matrix elements of $\mathbb{M}_{N,k}$ and $r_{k,k-1}$. The k-value to be used is that of the last medium (in the sense N, N-1, N-2. . . . . , k) to possess a non-vanishing reflected wave, E_k^-.

2.2 Calculation of Complex Index of Refraction

2.2.1 General Formulation

Since $\hat{n} = \sqrt{\hat{\epsilon}}$, the calculation of $\hat{n}$ is essentially one of calculating $\hat{\epsilon}$, which is defined by

$$\hat{\epsilon} = \frac{\hat{D}}{\hat{E}} = \frac{\hat{E} + 4\pi \hat{P}}{\hat{E}} = 1 + 4\pi \frac{\hat{P}}{\hat{E}}$$

where $\hat{P}$ is the electric polarization/unit volume induced by the electric field $\hat{E}$. If a sinusoidally varying electric field acts upon a bound electron of resonant frequency ω_q, then elementary treatments show that a dipole moment[5]

$$\hat{p} = \frac{e^2/m}{\omega_q^2 - \omega^2 + i\eta_q\omega}\,\hat{E}$$

is induced, where the $\eta_q\omega$-term arises from radiation damping. If there are n_q such bound electrons per unit volume, then

$$\hat{\epsilon} = 1 + \frac{4\pi e^2}{m}\,\frac{n_q}{\omega_q^2 - \omega^2 + i\eta_q\omega}$$

In separating $\hat{\epsilon}$ into its real and imaginary components, it is customary to express the real components as the sum of a fixed unit term and the deviation from unity:

$$\hat{\epsilon} = 1 - 2\delta - 2i\beta$$

so that the (reduced) real component δ is[5]

$$\delta_q(\omega) = \frac{2\pi e^2}{m}\,n_q\,\frac{(\omega^2 - \omega_q^2)}{(\omega_q^2 - \omega^2)^2 + \eta_q^2\omega^2}$$

For frequencies far beyond the resonance

$$\delta_q(\omega) \simeq \frac{2\pi e^2}{m}\,\frac{n_q}{\omega^2}$$

which, as the oscillator parameters ω_q and η_q are absent, is oscillator-model independent. The imaginary part, β,

since it occasions the imaginary component of the wave-vector, $\hat{\vec{k}}$, which in turn produces attenuation of the wave, is most directly associated with the linear attenuation coefficient[5]

$$\beta(\omega) = \frac{c}{2\omega}\,\mu(\omega)$$

A general treatment of $\hat{\epsilon} = 1 - 2\delta - 2i\beta$, based on dispersion relations, shows that[6]

$$\delta(\omega) = \frac{2}{\pi}\,\mathcal{P}\int_0^\infty \frac{\omega'\,\beta(\omega')\,d\omega'}{\omega^2 - \omega'^2}$$

$$\beta(\omega) = \frac{2\omega}{\pi}\,\mathcal{P}\int_0^\infty \frac{\delta(\omega')\,d\omega'}{\omega^2 - \omega'^2}$$

which, following of necessity from causality, are model independent. Comparing the high-frequency limit of this dispersion integral for $\delta(\omega)$ with that derived earlier

$$\delta_q(\omega) \simeq \frac{2\pi e^2}{m}\,\frac{n_q}{\omega^2}$$

$$\simeq \frac{2}{\pi\omega^2}\int_0^\infty \omega'\beta_q(\omega')\,d\omega'$$

or,

$$n_q = \frac{m}{\pi^2 e^2}\int_0^\infty \omega'\beta(\omega')\,d\omega'$$

This suggests defining a function $f_q(\omega)$[5]

$$f_q(\omega) = \frac{m}{\pi^2 e^2}\,\omega\beta(\omega) = \frac{mc}{2\pi^2 e^2}\,\mu(\omega)$$

such that

$$\int_0^\infty f_q(\omega)\,d\omega = n_q$$

The function $f_q(\omega)$ is called the "oscillator strength" density (per unit frequency per unit volume) for the electrons associated with the resonance at ω_q.

Accordingly, a general prescription for the real component, δ, is[5]

$$\delta(\omega) = \mathrm{Re}\left[\frac{2\pi e^2}{m} \int_0^\infty \frac{f_q(\omega')\, d\omega'}{\omega^2 - \omega'^2 - i\eta_q\omega}\right]$$

where the principal value of the dispersion integral has been implemented through the artifice of offsetting the pole at ω into the complex plane, analogous to the radiation damping term of the earlier treatment.

2.2.2 Specific Model for Absorption Coefficients

Empirically it is found that the frequency dependence of the absorption coefficient, $\mu_q(\omega)$, associated with the q^{th} atomic shell, is reasonably well approximated by the power function[7]

$$\mu_q(\omega) \simeq \mu_q \left(\frac{\omega}{\omega_q}\right)^{-p_q} U(\omega - \omega_q)$$

where

$$\mu_q = \mu_q(\omega_q)$$

$$\omega_q = \frac{1}{\hbar} \times (q^{th} \text{ shell binding energy})$$

p_q — empirically determined constant (of the order of 2 to 4)

and

$$U(x) = 1 \text{ for } x > 0$$
$$= 0 \text{ for } x < 0$$

In terms of this model

$$f_q(\omega) = \frac{m c}{2\pi^2 e^2} \mu_q(\omega) = \frac{m c \mu_q}{2\pi^2 e^2} \left(\frac{\omega}{\omega_q}\right)^{-p_q} U(\omega - \omega_q)$$

and

$$n_q = \int_0^\infty d\omega\, f_q(\omega) = \frac{m c \mu_q}{2\pi^2 e^2} \frac{\omega_q}{(p_q - 1)} \qquad (\text{for } p_q > 1)$$

so that

$$f_q(\omega) = \frac{p_q - 1}{\omega_q} n_q \left(\frac{\omega}{\omega_q}\right)^{-p_q} U(\omega - \omega_q)$$

and[7]

$$\mathcal{S}_q(\omega) = \frac{2\pi e^2}{m} \frac{p_q - 1}{\omega_q} n_q \, \mathrm{Re} \int_{\omega_q}^\infty \frac{\left(\frac{\omega'}{\omega_q}\right)^{-p_q} d\omega'}{\omega^2 - \omega'^2 - i\eta_q \omega}$$

Two normalizing modifications to this formulation prove to be convenient. If N is the number of atoms per unit volume, then g_q defined as

$$g_q = n_q / N$$

is the oscillator strength (of the q^{th} shell) per atom, whereas n_q is the oscillator strength per unit volume. Secondly, factoring out the known $1/\omega^2$ high frequency behavior of the integral yields

$$\mathcal{S}_q(\omega) = \frac{2\pi e^2}{m} \frac{N g_q}{\omega^2} (p_q - 1) \, \mathrm{Re}(I_q)$$

where

$$I_q = \frac{1}{\omega_q} \int_{\omega_q}^{\infty} \frac{\omega^2 \left(\frac{\omega'}{\omega_q}\right)^{-p_q} d\omega'}{(\omega^2 - \omega'^2 - i\eta_q \omega)}$$

Defining

$$x = \frac{\omega}{\omega_q} = \frac{\lambda_q}{\lambda}$$

$$v = \frac{\omega'}{\omega_q}$$

and

$$\zeta = \eta_q / \omega \quad \text{(generally} \lesssim 10^{-3,-4}\text{)}$$

then

$$I_q(p_q; x) = \int_1^{\infty} \frac{x^2 v^{-p_q} \, dv}{(x^2 - v^2 - i\zeta x^2)}$$

Letting $y = 1/v^2$

then

$$I_q(p_q; x) = \frac{1}{2(1 - i\zeta)} \int_0^1 \frac{y^{\frac{p_q - 1}{2}} \, dy}{\left[y - \frac{1}{x^2(1 - i\zeta)}\right]}$$

Further, defining

$$\xi = 1/x^2 (1 - i\zeta) = \left(\frac{\omega_q}{\omega}\right)^2 \frac{1}{(1 - i\zeta)}$$

$$\alpha = \frac{1}{2}(p_q - 1)$$

$$K = \frac{e^2 N}{2\pi m c^2} \quad (N = \text{number of atoms/unit volume})$$

and

$$J_q = (p_q - 1) I_q$$

one finally obtains[7]

$$\delta_q = K \lambda^2 g_q \, \mathrm{Re}\,[J_q(p_q;x)]$$

where explicitly

$$J_q(p_q;x) = \frac{\alpha}{(1 - i\beta)} \int_0^1 \frac{y^{\alpha}\, dy}{(y - \xi)}$$

This integral can be integrated analytically for certain (rational) values of p_q. The early Kramers[8] - Kallmann - Mark[9] treatment assumed a value of $p_q = 3$ and their results have been used extensively. Later, examining the effects of neglecting radiation damping, Parratt and Hempstead[7] obtained analytic integrations, correct to first order in β, for the cases $p_q = 2,\ 7/3,\ 2.5,\ 2.75,\ 3$ and 4 and prepared tables of the results evaluated over the range $0.01 \leq \lambda / \lambda_q \leq 15.0$. Also, they concluded that for ω / ω_q differing from unity by more than a part in 10^{-4}, neglect of radiation damping effects would produce a numerical error in the results of about a part in 10^{-3} or less.

2.2.3 Evaluation of the Integral $J_q(p_q;x)$

The total $\delta(\omega)$ being the sum of the partial $\delta_q(\omega)$'s characterizing each shell, together with the sum-rule (5) for oscillator strengths (i.e., $Z = \sum_q g_q$), results in

$$\begin{aligned}
\delta(\omega) &= \sum_q \delta_q(\omega) \\
&= K \lambda^2 \sum_q g_q \, \mathrm{Re}\,[J_q(p_q;x)] \\
&= K \lambda^2 \sum_q g_q \left\{ 1 + \mathrm{Re}\,[J_q(p_q;x)] - 1 \right\} \\
&= K \lambda^2 \left\{ Z + \sum_q g_q \, \mathrm{Re}\,[J_q(p_q;x) - 1] \right\}
\end{aligned}$$

with $K \lambda^2 Z$ being called the normal term and $K \lambda^2$ times the sum called the anomalous term. Thus, it is the quantity $\mathrm{Re}\,(J_q - 1)$ that is to be calculated and, neglecting the damping effects, this further reduces to

$$J_q(p_q;x) - 1 \simeq \alpha \int_0^1 \frac{y^\alpha \, dy}{y - \xi} - 1$$

where

$$\alpha = \frac{1}{2}\,[p_q - 1]$$

and

$$\xi = \frac{1}{x^2} = \left(\frac{\omega_q}{\omega}\right)^2 = \left(\frac{\lambda}{\lambda_q}\right)^2$$

This real integral is singular for $0 \leq \xi \leq 1$, the singularity being integrable, in the principal value sense, for $\xi \neq 1$. For $\xi > 1$, there is no singularity and a series solution is readily obtained:

$$J_q(p_q;x) = -1 - \alpha \sum_{h=1}^{\infty} \frac{x^{2n}}{(\alpha + n)}$$

For $0 \leq \xi < 1$, the situation is a bit more involved. For non-integer values of α (i.e., for p_q not equal to an odd integer) series expansion of the principal value integral yields the result

$$J_q(p_q;x) - 1 = \alpha \left[\sum_{n=1}^{\infty} \frac{1}{(\alpha - n)\, x^{2n}} - \pi \cot \pi\alpha \,/\, x^{2\alpha} \right]$$

which has obvious problems when α is an integer. If α is

equal to the integer k, then letting α approach the integer k as a limit gives

$$J_q(p_q;x) - 1 = k \left[\sum_{\substack{n=0 \\ (n \neq k)}}^{\infty} \frac{1}{(k-n)\, x^{2n}} + 2 \ln x / x^{2k} \right]$$

The programmed evaluation of the integral $J_q - 1$ proceeds as follows. If x is too close to unity for the series solutions to converge reasonably quickly, a 1000-point numerical integration is performed on an integrand similar to the original, complex one:

$$\int_0^1 \frac{y^{\alpha}\, dy}{y - \xi} \simeq \mathrm{Re} \int_0^1 \frac{y^{\alpha}\, dy}{y - \xi - i\eta}$$

$$= \int_0^1 \frac{(y - \xi)\, y^{\alpha}\, dy}{(y - \xi)^2 + \eta^2}$$

with η being set to 10^{-3}. When the integrand exceeds 100 (i.e., is close by the singularity), the integration step size of 10^{-3} is reduced to 10^{-4}. When the x-value is suitable for the series solutions, the series for $x < 1$ can be used without further consideration, but for $x > 1$ an additional decision must be made. If α differs from an integer by more than one part in 100, the non-integer α series is used. If α is closer than that to an integer, a zeroth order approximation, obtained from the integer α series, is improved with a numerical α -derivative times the difference between α and the integer. The numerical α -derivative is simply the difference

between the integral evaluated for α equal to the integer ± 0.01 (using the non-integer α series) divided by 0.02.

2.2.4 Composite Materials

2.2.4.1 Imaginary Component — β

If σ_i is the atomic absorption cross section for a type-i atom, N_i is the number of type-i atoms per unit volume, and V the volume in which the atoms were found, then the total absorption cross-section due to all type-i atoms is given by[10]

$$(\sigma_i)_{tot} = \sigma_i N_i V$$
$$= \mu_i V$$

where $\mu_i = \sigma_i N_i$ is the linear absorption coefficient for type-i atoms. Summing over all atomic species within volume V

$$\sigma_{mix} = \sum_i \sigma_i N_i V$$
$$= V \sum_i \mu_i$$
$$= V \mu_{mix}$$

Since $\frac{\mu}{\rho}$ is virtually independent of the physical state of the material, it is a more useful quantity to deal with.

$$\left(\frac{\mu}{\rho}\right)_{mix} = \frac{\mu_{mix}}{\rho_{mix}} = \frac{V}{M_{mix}} \sum_i \mu_i = \sum_i \frac{\mu_i}{\rho_i} \frac{\rho_i V}{M_{mix}}$$
$$= \sum_i \left(\frac{\mu}{\rho}\right)_i \frac{m_i}{M_{mix}}$$
$$= \sum_i f_i \left(\frac{\mu}{\rho}\right)_i$$

where

$$f_i = \frac{m_i}{m_{mix}} = \frac{m_i}{\sum_j m_j}$$

is the fraction (by mass) of the i^{th} atomic species. If a composite is known by its chemical formula — $(Z_1)_{n_1} (Z_2)_{n_2} \cdots\cdots$ (e.g. $Na_2 SO_4$) — then in terms of the elemental multiplicities, n_i, and atomic weights, A_i:

$$f_i = \frac{n_i A_i}{\sum_j n_j A_j}$$

Accordingly, for composite materials:

$$\beta_{mix}(\omega) = \frac{\lambda \rho_{mix}}{4\pi} \sum_i f_i \left(\frac{\mu(\omega)}{\rho}\right)_i$$

2.2.4.2 Real Component — δ

Essentially δ is a measure of the polarization per unit volume induced in an assembly of bound charges by an applied E-field. For the q-shell electrons in type-i atoms, the expression obtained earlier for δ becomes

$$\delta_{iq}(\omega) = K_i \lambda^2 g_{iq} \, \mathrm{Re}\left[J_q \left(p_{iq}, \frac{\omega}{\omega_{iq}}\right) \right]$$

where

$$K_i = \frac{e^2}{2\pi m c^2} N_i$$

and N_i is the number of type-i atoms per unit volume. In turn, N_i can be expressed as

$$N_i = N_o \rho_{mix} \frac{f_i}{A_i}$$

where

N_o - Avogadro's number

ρ_{mix} - density of composite material

f_i - fraction (by mass) of type-i atoms

A_i - atomic mass of type-i atoms

Thus, for composite materials

$$\delta_{mix}(\omega) = \sum_i \sum_q \delta_{iq}(\omega)$$

$$= \frac{e^2 N_o}{2\pi m c^2} \rho_{mix} \lambda^2 \sum_i \frac{f_i}{A_i} \times$$

$$\left\{ Z_i + \sum_q g_{iq} \, \mathrm{Re}\left[J_q\left(p_{iq}; \frac{\omega}{\omega_{iq}}\right) - 1 \right] \right\}$$

3.0 TESTS AND CHECK CASES

3.1 X-ray Reflection from Multilayer Surface

The program XREFL performs both numerical computations and certain layer data "book-keeping" functions. These two aspects can be tested separately and working together.

3.1.1 Substrate Alone

A good overall test of the computational parts of the program is to apply it to the case of a substrate with no layers on top. The computer results obtained for $\beta/\delta = 0$ as well as several cases with non-zero β/δ values agreed exactly with tables previously prepared from the general two-medium interface reflectance formula[5]:

$$R = \frac{[\sqrt{2}\ x - \sqrt{\alpha_+}\ ]^2 + \alpha_-}{[\sqrt{2}\ x + \sqrt{\alpha_+}\ ]^2 + \alpha_-}$$

where

$$x = \theta / \theta_c = \theta/\sqrt{2\delta}$$

$$y = \beta/\delta$$

and

$$\alpha_\pm = \sqrt{(x^2 - 1)^2 + y^2} \pm (x^2 - 1)$$

3.1.2 Substrate and Layer Materials Identical

A rough check of the "book-keeping" aspects of the program is to apply it to cases where the layer material is

the same as the substrate material — physically indistinguishable from a substrate without layers above. The results were, as to be expected, identical to those for the substrate alone.

3.1.3 Vacuum Layer Between Layer and Substrate of Identical Material

Let medium 3, the medium of the incident beam, be vacuum; medium 2 be of arbitrary material and thickness; medium 1 be vacuum, but of arbitrary thickness; and medium 0, the substrate, of the same material as medium 2. Then, there is only one basic reflection coefficient entering in:

$$r_{10} = \frac{n_1 \cos \phi_1 - n_o \cos \phi_o}{n_1 \cos \phi_i + n_o \cos \phi_o}$$

together with the respective layer phase shifts

$$\psi_n = \frac{2\pi}{\lambda} d_n n_n \cos \phi_n$$

In terms of these, it can be shown that[4]

$$r_{210} = r_{10} \frac{(e^{i(\psi 2 - \psi 1)} - e^{-i(\psi 2 - \psi 1)} + e^{-i(\psi 2 + \psi 1)} - r_{10}^2 e^{i(\psi 2 - \psi 1)}}{e^{i(\psi 2 + \psi 1)} - r_{10}^2 [e^{-i(\psi 2 - \psi 1)} - e^{-i(\psi 2 + \psi 1)} + e^{i(\psi 2 - \psi 1)}}$$

where

$$\psi_1 = \frac{2\pi d_1}{\lambda} n_1 \cos \phi_1 = \frac{2\pi d_1}{\lambda} \sqrt{n_1^2 - n_1^2 \sin^2 \phi_1}$$

$$= \frac{2\pi d_1}{\lambda} \sqrt{n_1^2 - n_3^2 \sin^2 \phi_3} \quad \text{(by Snell's Law)}$$

$$= \frac{2\pi d_1}{\lambda} \cos \phi_3 \quad \text{(since } n_1 = n_3 = 1 \text{ in vacuo)}$$

$$= \frac{2\pi d_1}{\lambda} \sin \theta_{inc}$$

$$\simeq \frac{2\pi d_1}{\lambda} \theta_{inc} \quad \text{(small angle approx.)}$$

and

$$\psi_2 = \frac{2\pi d_2}{\lambda} n_2 \cos \phi_2 = \frac{2\pi d_2}{\lambda} \sqrt{n_2^2 - n_2^2 \sin^2 \phi_2}$$

$$= \frac{2\pi d_2}{\lambda} \sqrt{n_2^2 - \sin^2 \phi_{inc}} = \frac{2\pi d_2}{\lambda} \sqrt{n_2^2 - 1 + \cos^2 \phi_{inc}}$$

$$= \frac{2\pi d_2}{\lambda} \sqrt{\sin^2 \theta_{inc} - (n_2^2 - 1)}$$

$$= \frac{2\pi d_2}{\lambda} \sqrt{\theta_{inc}^2 - 2\delta_2}$$

If the thickness d_1 of the vacuum layer is taken to be

$$d_1 = \frac{\lambda}{2\theta_{inc}}$$

then $\psi_1 = \pi$ and R reduces to $\left| r_{10} \right|^2$. Also, if the thickness d_2 of the material layer is taken to be

$$d_2 = \frac{\lambda}{d\sqrt{\theta_{inc}^2 - 2\delta_2}}$$

then $\psi_2 = \pi$ and R again reduces to $\left| r_{10} \right|^2$.

Testing these results, it was found that the reflectance table for the layer case agreed with the table for the substrate alone only at those angles of incidence for which:

1. ψ_1 is a multiple of π — and the results were the same for different material layer thicknesses, or,
2. ψ_2 is a multiple of π — and the results were the same for different vacuum layer thicknesses.

3.1.4 Linear Density Gradient above Substrate

In these cases, the layer material is the same as that of the substrate, but of differing density. The results for 0, 250Å and 500Å layers are shown in Figure 1. For a wavelength of $\lambda = 8.34$Å, the arbitrary (but not untypical) values of $\delta = 3.2 \times 10^{-4}$ and $\beta/\delta = 0.05$ were assumed. In the five-layer case, the layer

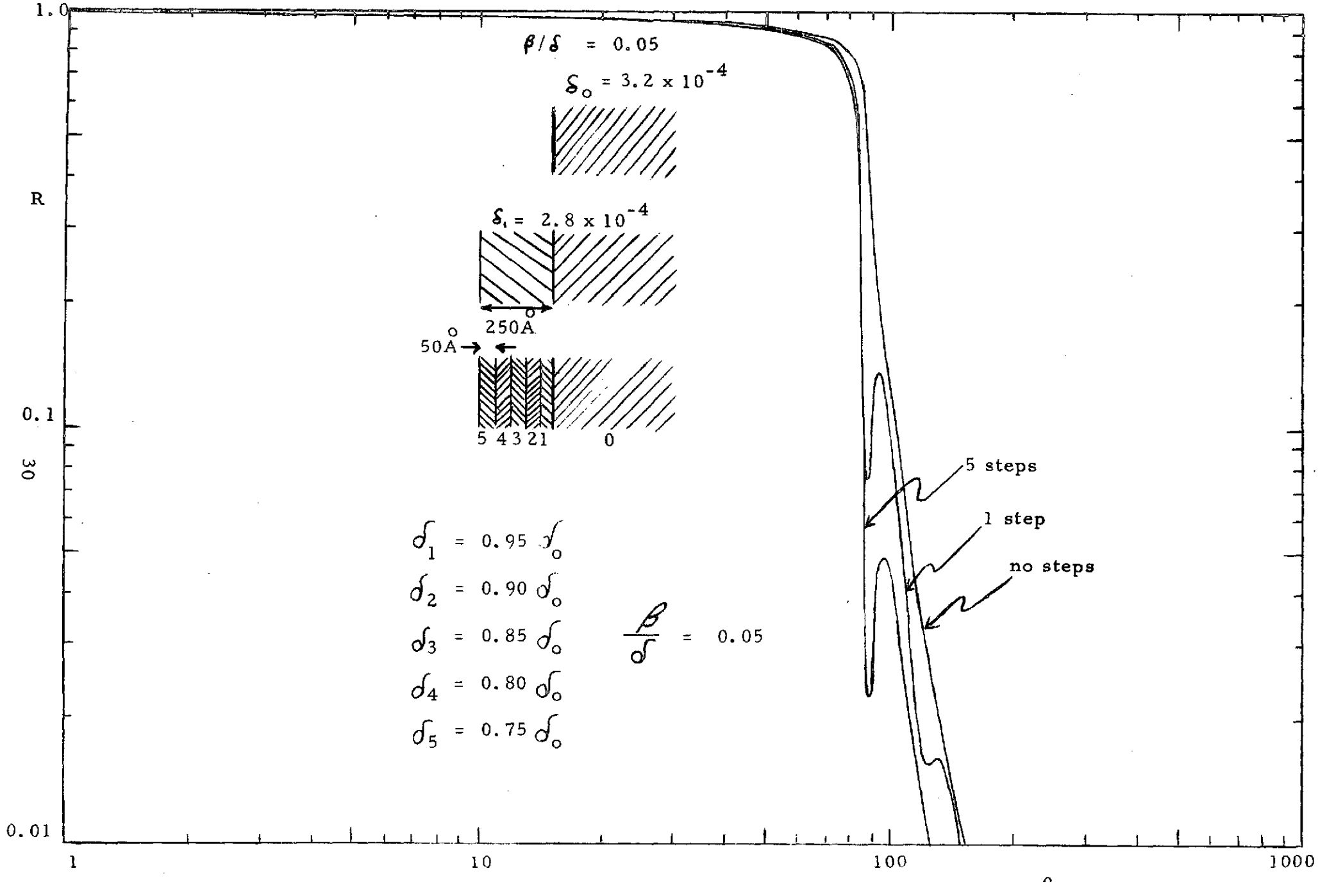
1.0
R
0.1
0.01
30
1
10
100
1000
β/δ = 0.05
δ₀ = 3.2 x 10⁻⁴
δ₁ = 2.8 x 10⁻⁴
250Å
50Å
5 4 3 2 1
0
δ₁ = 0.95 δ₀
δ₂ = 0.90 δ₀
δ₃ = 0.85 δ₀
δ₄ = 0.80 δ₀
δ₅ = 0.75 δ₀
β/δ = 0.05
5 steps
1 step
no steps

densities were chosen to approximate a linear density gradient — ρ_5, ρ_4, ρ_3, ρ_2 and ρ_1 were respectively 0.75, 0.80, 0.85, 0.90 and 0.95 times the substrate density. The layer β and δ values, being linearly proportional to the density, varied in similar fashion, with the β/δ ratio, of course, remaining fixed. In the single-layer case, the layer density was taken as an average of the layer no. 5 and substrate densities, i.e., 0.875 times the substrate density.

Qualitatively, the results are reasonable. The single-layer case has two pronounced interference maxima, and the five-layer case, a closer approximation to a linear density gradient, has but one maximum, substantially reduced in amplitude. In the single-layer case, there is a quantitative check that can be made concerning the separation of the interference maxima. The reflection coefficient for a single layer on a substrate is given by[3]

$$r = \frac{r_{21} + r_{10}\, e^{-2i\psi_1}}{1 + r_{21}\, r_{10}\, e^{-2i\psi_1}}$$

where r_{21} and r_{10} are the reflection coefficients for, respectively, the incidence medium/layer and layer/substrate interfaces, and ψ_1 is the phase shift of the layer

$$\psi_1 = \frac{2\pi d_1}{\lambda}\, n_1 \cos \phi_1$$

Since the medium was assumed to have a non-zero β_1 value, $n_1 \cos \phi_1$ will be complex:

$$n_1 \cos \phi_1 = U_R - iU_I$$

$$\simeq \sqrt{\theta_{inc}^2 - 2\delta_1 - 2i\beta_1}$$

where

$$2U_R^2 \simeq \sqrt{(\theta_{inc}^2 - 2\delta_1)^2 + 4\beta_1^2} + (\theta_{inc}^2 - 2\delta_1)$$

and

$$2U_I^2 \simeq \sqrt{(\theta_{inc}^2 - 2\delta_1)^2 + 4\beta_1^2} - (\theta_{inc}^2 - 2\delta_1)$$

The phase factor in the single-layer reflection formula then becomes

$$e^{-2i\psi_1} = e^{-\frac{4\pi d_1}{\lambda} U_I} e^{-i\frac{4\pi d_1}{\lambda} U_R}$$

Neglecting the relatively slower changes in r_{21} and r_{10} with respect to θ_{inc}, the maxima should correspond to $\mathrm{Re}(\delta\psi_1) = \pi \times \text{integer}$.

$$= \frac{2\pi d_1}{\lambda} \delta U_R$$

Accordingly, for two adjacent maxima,

$$\frac{2 d_1}{\lambda} \delta U_R = 1$$

or,

$$d_1 = \frac{\lambda}{2\delta U_R}$$

The single-layer maxima occur at about $\theta_{inc} = 94'$ and $\theta_{inc} = 130'$, for which the corresponding U_R values are 1.374×10^{-2} and 2.950×10^{-2} respectively. For $\lambda = 834\text{Å}$ and $\delta U_R = 1.576 \times 10^{-2}$, a layer thickness of $d_1 \simeq 265\text{Å}$ is predicted, in good agreement with the actual value of 250Å, the 6% discrepancy due probably both to errors in exact location of the maxima and to neglect of the angular variation on r_{21} and r_{10}.

3.1.5 Vacuum Deposition Density Profile Studies of Parratt

In a study of the effects of oxide layers and varying surface densities of vacuum deposition coatings, Parratt[11] presented some x-ray reflectance curves for copper, shown in Figure 2, corresponding to various multilayer approximations to certain hypothesized surface density profiles. Using the input data of his Cases I and III (exhibiting the most pronounced behavior) the computer program produced the results shown in Figures 3 and 4, agreeing, evidently, quite well with Parratt's results.

3.1.6 Numerical Test Point

One final quantitative check was made by "hand calculating" a single reflectance value for a three-layer case whose parameters were chosen so as not to have any obvious "small integer" relationships. The hand calculation and corresponding computer results agreed to five significant places.

3.2 Calculations of Complex Index of Refraction

The programs for calculating the δ and β components of the complex index of refraction likewise contain computational and data book-keeping aspects which can be tested separately and working together.

3.2.1 The Integral $J_q - 1$

The central calculation in computing the complex index of refraction is that of the integral $J_q\ (p;x) - 1$. The tables of Parratt and Hempstead[7] mentioned earlier provide an extensive and yet convenient check — after weeding out a number of bad entries. Upon encountering several perplexing, randomly occurring discrepencies

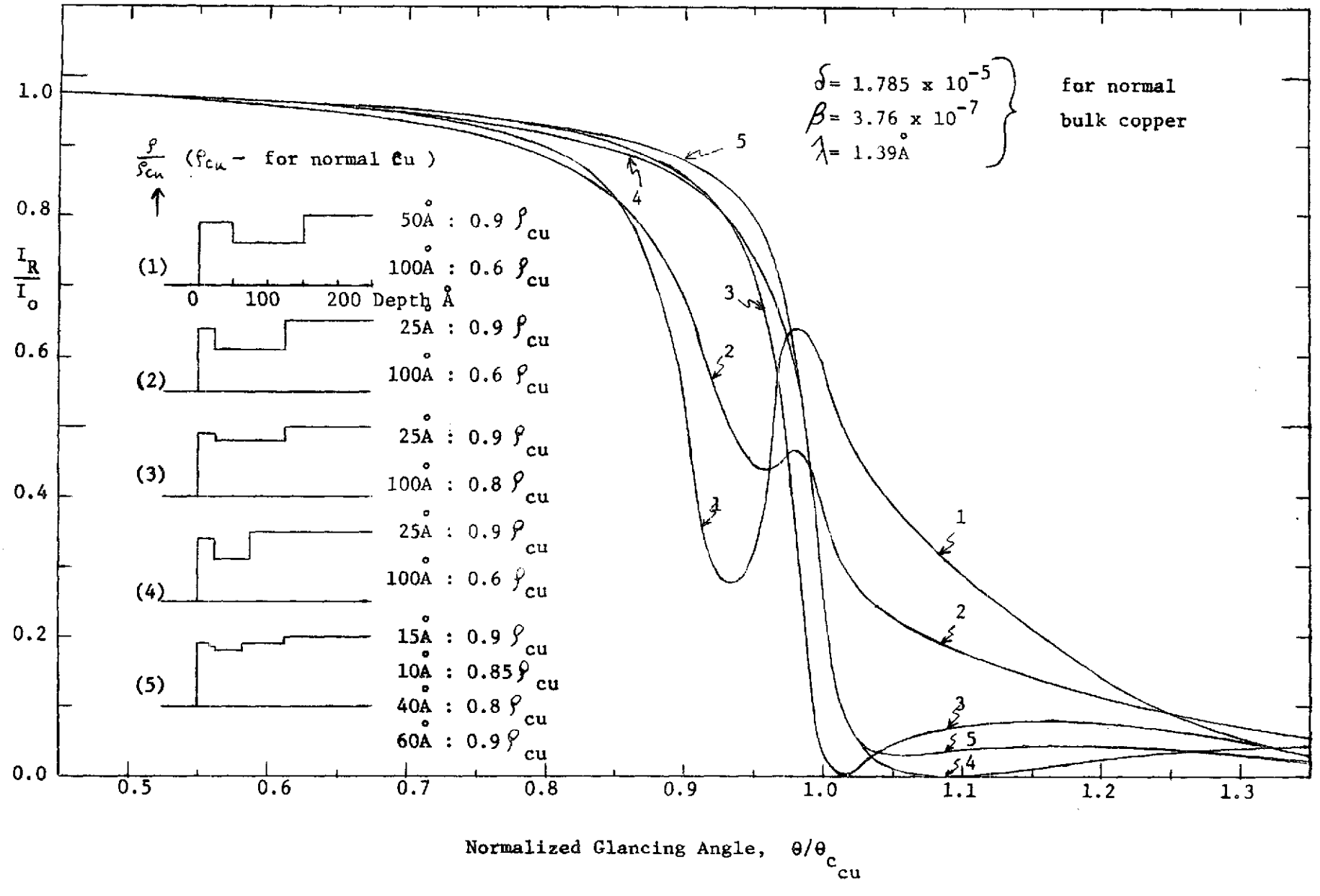
(Curves taken from L.G. Parratt,
Phys. Rev. 95, 359 (1954))
δ = 1.785 x 10^-5
β = 3.76 x 10^-7
λ = 1.39Å
for normal
bulk copper
ρ/ρcu (ρcu - for normal Cu)
(1) 50Å : 0.9 ρcu
100Å : 0.6 ρcu
0 100 200 Depth Å
(2) 25Å : 0.9 ρcu
100Å : 0.6 ρcu
(3) 25Å : 0.9 ρcu
100Å : 0.8 ρcu
(4) 25Å : 0.9 ρcu
100Å : 0.6 ρcu
(5) 15Å : 0.9 ρcu
10Å : 0.85 ρcu
40Å : 0.8 ρcu
60Å : 0.9 ρcu
I_R / I_o
1.0
0.8
0.6
0.4
0.2
0.0
0.5 0.6 0.7 0.8 0.9 1.0 1.1 1.2 1.3
Normalized Glancing Angle, θ/θc_cu

FIGURE 2.

C.F. Parratt, PR 95, 359 (1954)

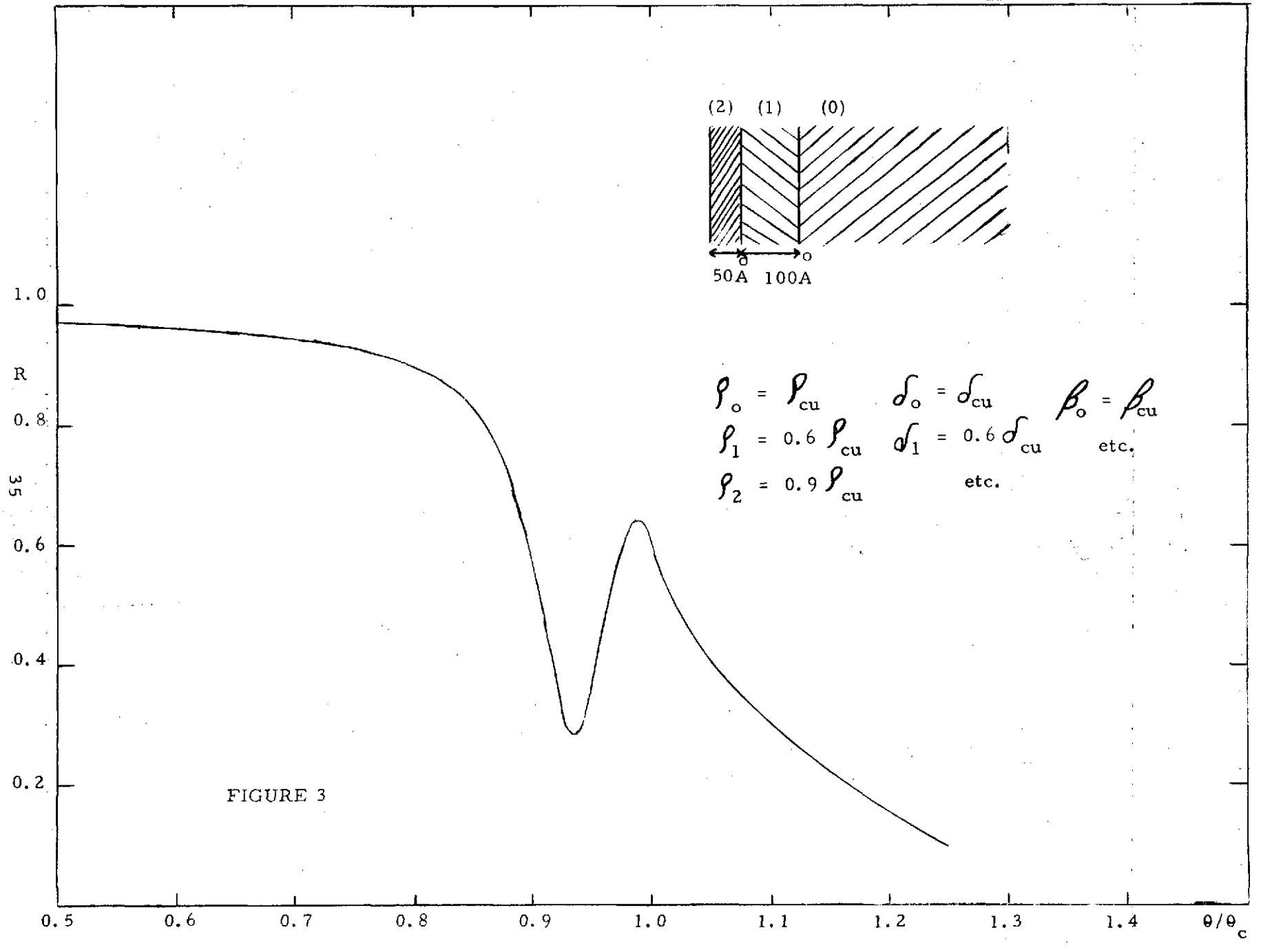

FIGURE 3

C. F. Parratt, PR 95, 359, (1954)

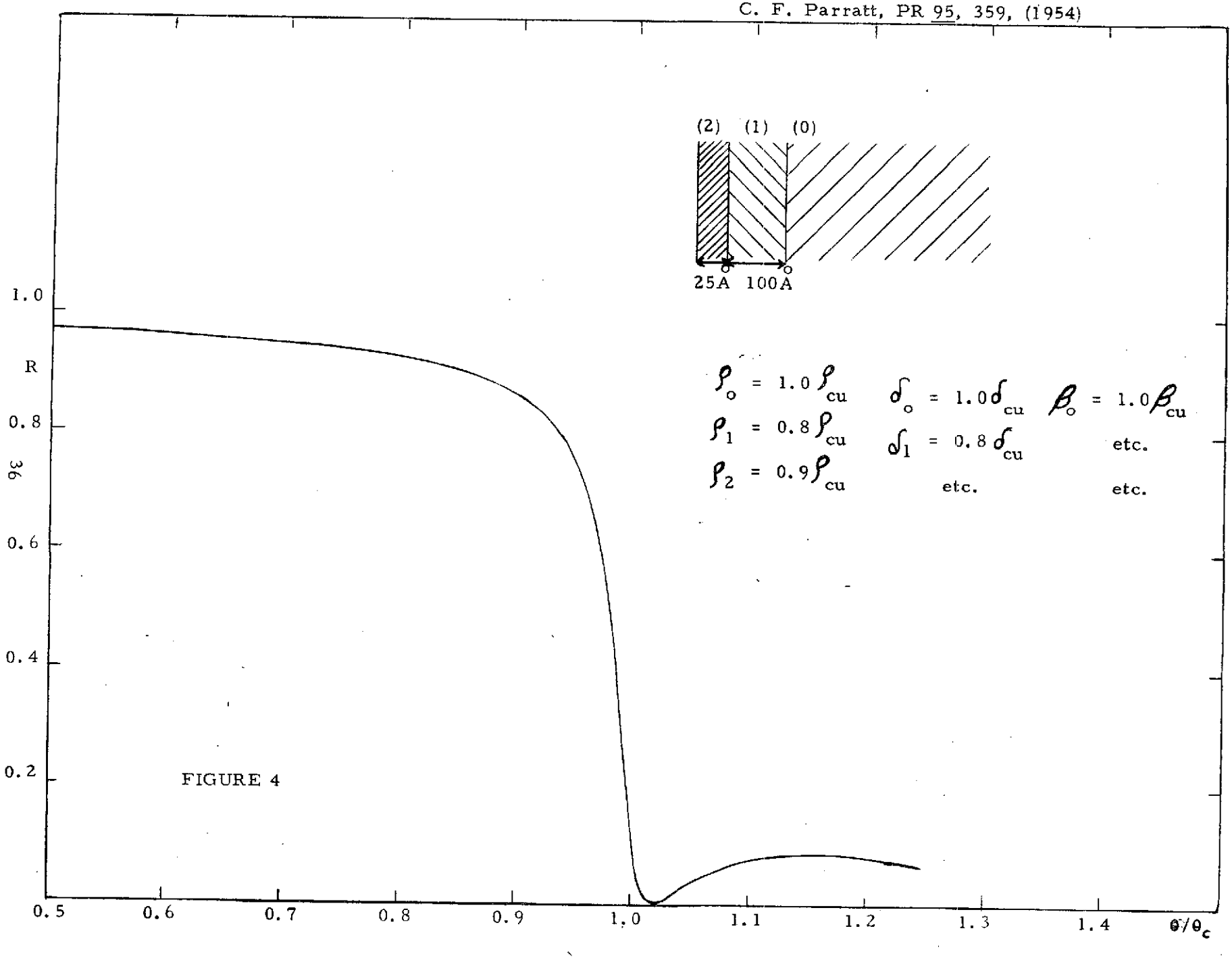

FIGURE 4

between table and computed values (amidst many accurate agreements), it became necessary to write a small program to evaluate the closed-form analytical expressions of Parratt and Hempstead for (p = 2, 7/3, 2.5, 2.75, 3 and 4), and a table similar to theirs was produced (Table 1). In the few entries having four significant digits, agreement was generally four-place. In the two- and three-digit entries there were many small (last digit) and a few large (first digit) errors, due presumably, to extensive desk-top calculator evaluations of the rather involved expressions. At any rate, the series or numerical integration values agreed very well with the special p-value function evaluations.

3.2.2 Values of β and δ

Since β for a composite material is basically a mass-fraction weighted average of input data (μ/ρ values), checking is trivial. For δ, four-place agreement was obtained with the value reported by Parratt[11] for the pure element copper, and the value reported in the NAS8-27605 Final Report for the compound material silica glass (SiO_2), thereby checking out the book-keeping aspects.

λ/λ_0	p = 2.0	p = 7/3	p = 5/2	p = 11/4	p = 3.0	p = 4.0
1.01	-1.000E-04	2.405E-03	2.056E-03	1.399E-03	9.210E-04	3.000E-04
1.03	-9.003E-04	9.471E-03	9.543E-03	8.051E-03	6.311E-03	2.698E-03
1.05	-2.502E-03	1.727E-02	1.884E-02	1.758E-02	1.497E-02	7.481E-03
1.10	-1.003E-02	3.608E-02	4.445E-02	4.794E-02	4.595E-02	2.970E-02
1.20	-4.055E-02	6.061E-02	8.976E-02	1.156E-01	1.271E-01	1.151E-01
1.30	-9.286E-02	5.857E-02	1.120E-01	1.704E-01	2.082E-01	2.449E-01
1.40	-1.695E-01	2.226E-02	9.918E-02	1.934E-01	2.653E-01	3.987E-01
1.50	-2.747E-01	-5.681E-02	3.921E-02	1.666E-01	2.747E-01	5.440E-01
1.60	-4.159E-01	-1.909E-01	-8.364E-02	6.802E-02	2.071E-01	6.308E-01
1.65	-5.039E-01	-2.845E-01	-1.760E-01	-1.797E-02	1.320E-01	6.288E-01
1.70	-6.071E-01	-4.010E-01	-2.950E-01	-1.362E-01	1.960E-02	5.775E-01
1.75	-7.297E-01	-5.464E-01	-4.481E-01	-2.959E-01	-1.414E-01	4.561E-01
1.80	-8.789E-01	-7.310E-01	-6.467E-01	-5.114E-01	-3.682E-01	2.325E-01
1.85	-1.067E+00	-9.728E-01	-9.121E-01	-8.081E-01	-6.914E-01	-1.468E-01
1.90	-1.325E+00	-1.311E+00	-1.289E+00	-1.240E+00	-1.174E+00	-7.897E-01
1.95	-1.740E+00	-1.868E+00	-1.917E+00	-1.972E+00	-2.008E+00	-2.004E+00
1.98	-2.252E+00	-2.559E+00	-2.698E+00	-2.889E+00	-3.062E+00	-3.606E+00
2.02	-2.354E+00	-2.722E+00	-2.895E+00	-3.144E+00	-3.380E+00	-4.225E+00
2.05	-1.950E+00	-2.195E+00	-2.308E+00	-2.469E+00	-2.619E+00	-3.141E+00
2.10	-1.674E+00	-1.840E+00	-1.916E+00	-2.021E+00	-2.119E+00	-2.448E+00
2.15	-1.531E+00	-1.657E+00	-1.714E+00	-1.794E+00	-1.866E+00	-2.107E+00
2.20	-1.439E+00	-1.541E+00	-1.587E+00	-1.650E+00	-1.707E+00	-1.895E+00
2.25	-1.373E+00	-1.459E+00	-1.497E+00	-1.549E+00	-1.596E+00	-1.750E+00
2.30	-1.324E+00	-1.397E+00	-1.429E+00	-1.474E+00	-1.514E+00	-1.643E+00
2.40	-1.254E+00	-1.310E+00	-1.335E+00	-1.369E+00	-1.399E+00	-1.495E+00
2.50	-1.207E+00	-1.252E+00	-1.272E+00	-1.299E+00	-1.323E+00	-1.398E+00
2.70	-1.147E+00	-1.178E+00	-1.192E+00	-1.210E+00	-1.227E+00	-1.278E+00
3.00	-1.098E+00	-1.119E+00	-1.128E+00	-1.140E+00	-1.150E+00	-1.183E+00
3.50	-1.059E+00	-1.071E+00	-1.076E+00	-1.083E+00	-1.089E+00	-1.108E+00
4.00	-1.039E+00	-1.047E+00	-1.051E+00	-1.055E+00	-1.060E+00	-1.072E+00
5.00	-1.013E+00	-1.016E+00	-1.017E+00	-1.019E+00	-1.020E+00	-1.024E+00
6.00	-1.003E+00	-1.004E+00	-1.004E+00	-1.004E+00	-1.005E+00	-1.006E+00
7.00	-1.001E+00	-1.001E+00	-1.001E+00	-1.002E+00	-1.002E+00	-1.002E+00

Table 1

4.0 PROGRAM OUTPUTS

The program always returns printed output, and optionally returns plotted graphical output.

4.1 Printed Output

The printed output consists of two main sections. In the first section, the input data is reproduced with appropriate labelling. In the second section, the calculated results are presented in tabular form.

4.1.1 Input data

The contents of the case label card are printed at the top of the page. Just below will be the general run parameters:

1. the in vacuo incident wavelength
2. the number of layers above the substrate (always layer no. 0)
3. the number of incidence angle/reflectance value tabular entries to be calculated
4. the minimum incidence angle to be used in the table
5. the incidence angle increment per tabular entry, and
6. the choice of plotted return or not

Then, layer by layer (topmost layer with highest index, substrate with zero index), the layer parameters are presented:

1. the depth or thickness of the layer
2. the layer material density, and
3. the number of atomic elements of which the layer material consists.

For a given layer, the parameters of each of the constituent atoms are successively presented:

1. the atomic number
2. the atomic weight
3. the fractional (by mass) abundance of the element in the layer material
4. the mass absorption coefficient, μ/ρ, at the specified incident wavelength
5. the number of atomic shells sufficing to describe the inner atom, and
6. the atomic shell parameters
   a) the shell index (NB a single index can refer to one level, e.g., L_I, or to a group, e.g., $M_I \rightarrow M_V$
   b) the shell absorption edge wavelength
   c) the exponent of the power-law dependence of the shell's contribution to the total μ/ρ, and
   d) the oscillator strength (per atom) of the shell.

4.1.2 Calculated Results

The contents of the case label card are printed at the top of the page, and just below, in vacuo incident wavelength is repeated. This is followed by a table of the layer parameters required for calculating the reflectance:

1) the layer thickness
2) the computed δ-value, and
3) the computed β-value.

This, in turn, is followed by the table of reflectance values consisting of

1) the angle of incidence (in arc minutes)
2) the (same) angle of incidence (in radians)
3) the reflectance value, and
4) the stopping layer

The stopping layer is defined as that layer in which the total attenuation (due both to inter-layer reflection and intra-layer absorption) of the incident beam field strength exceeds 10^4. Total reflection by a layer is interpreted as the beam stopping within that layer. At zero-incidence angle, there is no penetration (similar to the case of total reflection) and the top-layer index is arbitrarily assigned as the stopping layer. Finally, in the case of the substrate, the value -1 is used to signify net transfer of beam power into the substrate (whether subsequently absorbed or transmitted) and the value 0 to signify total reflection from the substrate.

4.2 Plotted Graphical Output

When the plot index is set to 1 (a plot is desired), the incidence angle/reflectance value table is transmitted to a plotting program package (drawing upon standard CALCOMP software) consisting of GOPLT, which is a plotter initializing routine; FRMPLT, which determines internal scaling values, draws a graph frame with tick marks and labels it; CRVPLT, which plots the reflectance vs. angle table; and ENDPLT which closes out the plotting routines.

Since each computation center has its own plotter conventions, GOPLT makes a call to a subroutine PLTID3, which transmits two arguments — a six-character BCD word (to identify user's plotted output) and an overall scale factor (a value of 1.0 producing output with an 8 1/2" x 11" format as indicated by the bounding tick marks). The

subroutine PLTID3 is best written by a systems programmer who knows the computation center conventions and should perform the following tasks:

1. make a call to PLOTS to define the output device and a PLOT working buffer
2. space the plotter away from previous user's plot results
3. label the plotter paper with the present user's six-character BCD ID word
4. define a new origin: 0.5" or more away from user label and 0.5" up from paper's edge, and
5. RETURN to GOPLT.

5.0 INPUT DATA FORMAT AND DECK SETUP

The general data deck consists of the data for an arbitrary number of cases (each case being a reflectance vs. angle curve for a given set of layer material data) followed by a "***END OF DATA***" card. The structure of a general data deck is given in Figure 5. The structure of a partial deck for a single case is as follows:

I. Case Label Card

Cols.	Format	Item
1 - 72	12A6	Arbitrary case identification data (e.g., date, specimen description, etc)

II. General Case Parameter Card

Cols.	Format	Item
1 - 10	E10.3	In vacuo incident wavelength (Angstroms)
14 - 15	I2	Number of layers above substrate (0 or more - up to 20)
18 - 20	I3	Number of reflectance table entries to be calculated (1 or more - up to 300)
21 - 30	E10.3	Initial incidence angle value (arc min.)
31 - 40	E10.3	Incidence angle increment (arc min.)
45	I1	Plotted result index (1 = YES, 0 = NO)

followed by layer description subdecks (1 or more - up to 20), containing

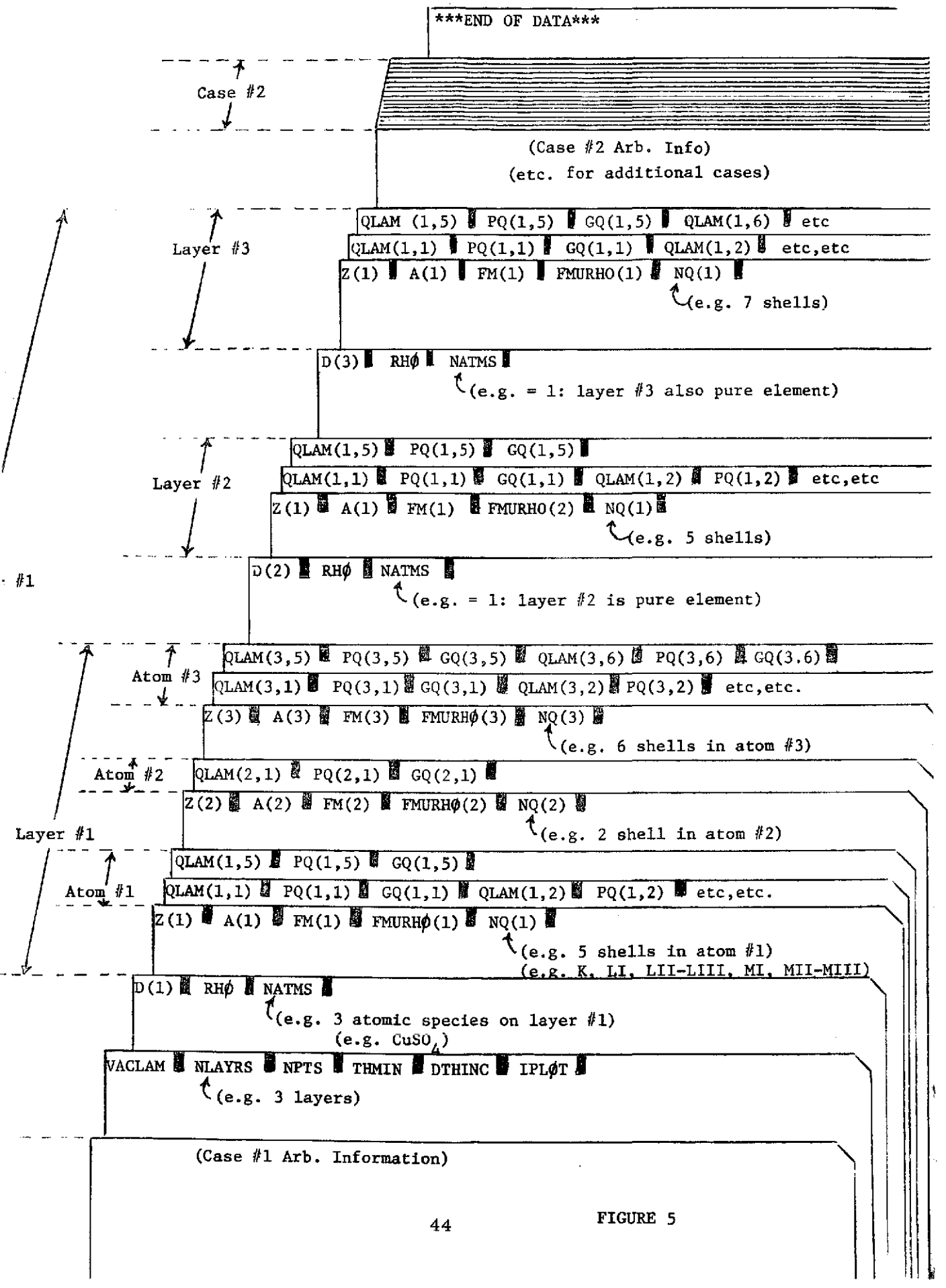
END OF DATA
Case #2
(Case #2 Arb. Info)
(etc. for additional cases)
Layer #3
QLAM (1,5) PQ(1,5) GQ(1,5) QLAM(1,6) etc
QLAM(1,1) PQ(1,1) GQ(1,1) QLAM(1,2) etc,etc
Z(1) A(1) FM(1) FMURHO(1) NQ(1)
(e.g. 7 shells)
D(3) RHØ NATMS
(e.g. = 1: layer #3 also pure element)
Layer #2
QLAM(1,5) PQ(1,5) GQ(1,5)
QLAM(1,1) PQ(1,1) GQ(1,1) QLAM(1,2) PQ(1,2) etc,etc
Z(1) A(1) FM(1) FMURHO(2) NQ(1)
(e.g. 5 shells)
#1
D(2) RHØ NATMS
(e.g. = 1: layer #2 is pure element)
Atom #3
QLAM(3,5) PQ(3,5) GQ(3,5) QLAM(3,6) PQ(3,6) GQ(3.6)
QLAM(3,1) PQ(3,1) GQ(3,1) QLAM(3,2) PQ(3,2) etc,etc.
Z(3) A(3) FM(3) FMURHØ(3) NQ(3)
(e.g. 6 shells in atom #3)
Atom #2
QLAM(2,1) PQ(2,1) GQ(2,1)
Z(2) A(2) FM(2) FMURHØ(2) NQ(2)
(e.g. 2 shell in atom #2)
Layer #1
QLAM(1,5) PQ(1,5) GQ(1,5)
Atom #1
QLAM(1,1) PQ(1,1) GQ(1,1) QLAM(1,2) PQ(1,2) etc,etc.
Z(1) A(1) FM(1) FMURHØ(1) NQ(1)
(e.g. 5 shells in atom #1)
(e.g. K, LI, LII-LIII, MI, MII-MIII)
D(1) RHØ NATMS
(e.g. 3 atomic species on layer #1)
(e.g. $CuSO_4$)
VACLAM NLAYRS NPTS THMIN DTHINC IPLØT
(e.g. 3 layers)
(Case #1 Arb. Information)

FIGURE 5

III. General Layer Parameter Card

Cols.	Format	Item
1 - 10	E10.3	Layer thickness (Angstroms)
11 - 20	E10.3	Layer material density (g/cm^3)
24 - 25	I2	Number of chemical elements in layer material (1 or more — up to 10)

followed by element description subdecks (1 or more — up to 10), containing

IV. Atomic Element Parameter Card

Cols.	Format	Item
1 - 5	F5.2	Atomic number of element
6 - 10	F5.2	Atomic weight of element (g/mole)
11 - 20	E10.3	Element abundance (mass fraction)
21 - 30	E10.3	Mass absorption coefficient $\frac{\mu}{\rho}$ (cm^2/g)
35	I1	Number of atomic shells (1 or more — up to 8)

followed by

V. Atomic Shell Parameter Cards (1 or 2)

Cols.	Format	Item
1 - 8	E8.2	Shell 1 absorption edge (Angstroms)
9 - 13	F5.2	Shell 1 absorption coefficient power law exponent (positive)
14 - 18	F5.2	Shell 1 oscillator strength (per atom)
19 - 26	E8.2	Shell 2 absorption edge (Angstroms)

27 - 31	F5.2	Shell 2 absorption coefficient power law exponent (positive)
32 - 36	F5.2	Shell 2 oscillator strength (per atom)
37 - 44	E8.2	Shell 3 absorption edge (Angstroms)

etc., etc.

NB No second atomic shell parameter card is required if the layer material consists of 4 or less atomic elements.

In order that computer system run termination diagnostics not be printed immediately below the last output value table (but rather on a new page), the last card in the data deck must be one containing the characters ***END OF DATA*** In colums 1 - 17.

6.0 PROGRAM LISTING

The program listing is given in the following data sheets.

```
      PROGRAM REFLTBL (INPUT,OUTPUT)
C     MAIN PROGRAM TO COMPUTE THE GLANCING X-RAY REFLECTIVITY VS.
C     ANGLE OF INCIDENCE FOR A LAMINATED SURFACE. THE BETA AND DELTA
C     ELEMENTS OF THE COMPLEX INDEX OF REFRACTION ARE CALCULATED
C     FOR EACH LAYER.
C
      DIMENSION TITLE(12),NLR(21),D(20),Z(10),A(10),FM(10),FMURHO(10),
     +  NQ(8),QLAM(10,8),PQ(10,8),GQ(10,8),THINCM(300),R2(300),
     +  DELTA(21),BETA(21)
      PRINT 200
  200 FORMAT(1H1)
      IPLT = 0
    1 READ 100, (TITLE(I),I=1,12)
  100 FORMAT(12A6)
      IF(TITLE(1).NE.6H***END) GO TO 5
      IF(IPLT.NE.0) CALL ENDPLT
      CALL EXIT
    5 READ 101, VACLAM,NLAYRS,NPTS,THMIN,DTHINC,IPLOT
  101 FORMAT(E10.3,3X,I2,2X,I3,2E10.3,4X,I1)
      PRINT 201,(TITLE(I),I=1,12),VACLAM,NLAYRS,NPTS,THMIN,DTHINC,IPLOT
  201 FORMAT(6X,12A6,///6X,13HLAMDA(VAC.) =,E10.3,10H ANGSTROMS,//
     +  6X,12HNO. LAYERS =,I3,//6X,15HNO. CALC. PTS =,I4/6X,6HINIT. ,
     +  6HANG. =,E10.3,9H ARC MIN.,/6X,12HANG. INCR. =,E10.3,
     +  9H ARC MIN.,//6X,19HPLOT(1=YES,0=NO) =,I2)
      IF(IPLOT.NE.0) IPLT = IPLT + 1
      IF(IPLT.EQ.1.AND.IPLOT.EQ.1) CALL GOPLT(6HID WRD,1.0)
      NLR1 = NLAYRS + 1
      DO 20 IL = 1,NLR1
      NLR(IL) = NLR1 - IL
      READ 102, D(IL),RHO,NATMS
  102 FORMAT(2E10.3,3X,I2)
      PRINT 202, NLR(IL),D(IL),RHO,NATMS
  202 FORMAT(///6X,5HLAYER,I3,15H PARAMETERS.....,//8X,7HDEPTH =,
     +  E10.3,10H ANGSTROMS,/8X,7HDENS. =,E10.3,6H G/CM3,/8X,
     +  20HNO. AT. COMPONENTS =,I3)
      DO 10 IA = 1,NATMS
      READ 103, Z(IA),A(IA),FM(IA),FMURHO(IA),NQ(IA)
  103 FORMAT(2F5.2,2E10.3,4X,I1)
      PRINT 203, IA,Z(IA),A(IA),FM(IA),FMURHO(IA),NQ(IA)
  203 FORMAT(/8X,9HCOMPONENT,I3,15H PARAMETERS.....,//10X,3HZ =,F5.0,
     +  /10X,3HA =,F6.1/10X,13HMASS FRACT. =,E10.3/10X,6HMU/RHO,
     +  9H(LAMDA) =,E10.3,6H CM2/G,/10X,16HNO. AT. SHELLS =,I2)
      NSHELS = NQ(IA)
      READ 104, (QLAM(IA,IS),PQ(IA,IS),GQ(IA,IS),IS=1,NSHELS)
  104 FORMAT(4(E8.2,2F5.2))
   10 PRINT 204, (IS,QLAM(IA,IS),PQ(IA,IS),GQ(IA,IS),IS=1,NSHELS)
  204 FORMAT(/10X,27HATOMIC SHELL PARAMETERS.....,//14X,1HQ,4X,
     +  8HLAMDA(Q),5X,4HP(Q),6X,4HG(Q),/18X,11H(ANGSTROMS),//8(14X,
     +  I1,3X,E10.3,F9.3,F9.2/))
      DELTA(IL) = FDELTA(VACLAM,RHO,NATMS,Z,A,FM,NQ,QLAM,PQ,GQ)
   20 BETA(IL) = FBETA(VACLAM,RHO,NATMS,FM,FMURHO)
```

```
      PRINT 205, (TITLE(I),I=1,12)
  205 FORMAT(1H1,5X,12A6)
      IF(NLAYRS.NE.0) GO TO 30
      PRINT 206, VACLAM,NLAYRS
  206 FORMAT(//6X,13HLAMDA(VAC.) =,E10.3,10H ANGSTROMS,//6X,5HREFL.,
     +  18H PARAMETERS OF THE,I3,11H LAYERS....,//8X,5HLAYER,3X,
     +  9HTHICKNESS,7X,5HDELTA,9X,4HBETA,/9X,3HNO.,3X,11H(ANGSTROMS),
     +  //20(9X,I2,3E14.3,/))
      PRINT 207
  207 FORMAT(7X,6H(NONE),//1X)
      GO TO 40
   30 PRINT 206, VACLAM,NLAYRS,(NLR(I),D(I),DELTA(I),BETA(I),
     +  I=1,NLAYRS)
   40 PRINT 208, DELTA(NLR1),BETA(NLR1)
  208 FORMAT(6X,21HAND THE SUBSTRATE....,//10X,1H0,14X,2E14.3)
      PRINT 209
  209 FORMAT(/////6X,31HTABLE OF REFLECTANCE VALUES....,////12X,
     +  11HTHETA(INC.),10X,11HREFLECTANCE,3X,8HSTOPPING,/6X,5H(ARC ,
     +  5HMIN.),3X,9H(RADIANS),21X,5HLAYER,/1X)
      NPTS1 = NPTS + 1
      DO 50 N = 1,NPTS1
      THINCM(N) = THMIN + FLOAT(N - 1)*DTHINC
      THINC = 2.90888E-4*THINCM(N)
      CALL XREFL(THINC,VACLAM,NLAYRS,D,DELTA,BETA,R2(N),NREFL)
   50 PRINT 210, THINCM(N),THINC,R2(N),NREFL
  210 FORMAT(8X,F5.1,2E15.3,I9)
      PRINT 200
      IF(IPLOT.EQ.0) GO TO 1
      THMAX = THMIN + FLOAT(NPTS)*DTHINC
      CALL FRMPLT(THMIN,THMAX,0,-0.1,1.1,THINCM,R2,NPTS1)
      CALL CRVPLT(THINCM,R2,NPTS1,1H ,0)
      GO TO 1
      END
```

```
      FUNCTION FDELTA(VACLAM,RHO,NATMS,Z,A,FM,NQ,QLAM,PQ,GQ)
      DIMENSION Z(10),A(10),FM(10),NQ(10),QLAM(10,8),PQ(10,8),GQ(10,8)
      ASUM = 0.0
      DO 20 IA = 1,NATMS
      QSUM = 0.0
      NQIA = NQ(IA)
      DO 10 IQ = 1,NQIA
      IF(GQ(IA,IQ).EQ.0.0) GO TO 10
      QSUM = QSUM + GQ(IA,IQ)*FJQL1(PQ(IA,IQ),QLAM(IA,IQ)/VACLAM)
   10 CONTINUE
   20 ASUM = ASUM + FM(IA)*(Z(IA) + QSUM)/A(IA)
      FDELTA = 2.70200E-6*RHO*VACLAM**2*ASUM
      RETURN
      END



      FUNCTION FBETA(VACLAM,RHO,NATMS,FM,FMURHO)
      DIMENSION FM(10),FMURHO(10)
      SUM = 0.0
      DO 10 I = 1,NATMS
   10 SUM = SUM + FM(I)*FMURHO(I)
      FBETA = 7.95775E-10*VACLAM*RHO*SUM
      RETURN
      END



      FUNCTION FJQL1(P,X)
      IF(P.GT.1.0) GO TO 20
      PRINT 100
   00 FORMAT(////23H ***** P IS LESS THAN 1,////)
   10 FJQL1 = 0.0
      RETURN
   20 IF(X.GT.1.0E3) GO TO 10
      FJQL1 = -1.0
      IF(X.LT.1.0E-2) RETURN
      ALPH = (P - 1.0)/2.0
      XI = 1.0/X**2
      IF(X.LT.0.5) FJQL1 = FJXLO(ALPH,XI)
      IF(X.GT.1.1) FJQL1 = FJXHI(ALPH,XI)
      IF(X.GE.0.5.AND.X.LE.1.1) FJQL1 = FJNUM(ALPH,XI)
      RETURN
      END
```

```
      FUNCTION FJNUM(A,XI)
      F(Y) = (Y - XI)*Y**A/((Y - XI)**2 + 1.0E-6)
      YN = 0.0
      DY = 1.0E-3
      FINT = 0.0
      DO 20 ISUM = 1,500
      FN0 = F(YN)
      FN1 = F(YN + DY)
      FN2 = F(YN + 2.0*DY)
      IF(AMAX1(ABS(FN0),ABS(FN1),ABS(FN2)).GT.1.0E2) GO TO 30
      FINT = FINT + FN0 + 4.0*FN1 + FN2
   10 YN = FLOAT(ISUM)*2.0*DY
   20 CONTINUE
      FJNUM = A*FINT*DY/3.0 - 1.0
      RETURN
   30 FINT1 = 0.0
      YN1 = YN
      DO 40 ISUM1 = 1,10
      FN0 = F(YN1)
      FN1 = F(YN1 + 0.1*DY)
      FN2 = F(YN1 + 0.2*DY)
      FINT1 = FINT1 + FN0 + 4.0*FN1 + FN2
   40 YN1 = YN + FLOAT(ISUM1)*0.2*DY
      FINT = FINT + FINT1*0.1
      GO TO 10
      END
```

```
      FUNCTION FJXLO(A,XI)
      SUM = 1.0/((A + 10.0)*XI)
      DO 10 I = 1,9
   10 SUM = (SUM + 1.0/(A + FLOAT(10 - I)))/XI
      FJXLO = -A*SUM - 1.0
      RETURN
      END
```

```
      FUNCTION FJXHI(A,XI)
      FN = IFIX(A + 0.5)
      EPS = A - FN
      IF(ABS(EPS).LT.0.01) GO TO 10
      FJXHI = FJA(A,XI)
      RETURN
   10 FJXHI = FJN(FN,XI) + (FJA(FN + 0.01,XI) - FJA(FN - 0.01,XI))
     +   *EPS/0.02
      RETURN
      END
```

```
      FUNCTION FJN(FN,XI)
      FJN = -1.0
      IF(FN.GE.11.0) RETURN
      SUM = XI/(FN + 26.0)
      DO 10 I = 1,25
      FNLI = FN + FLOAT(26 - I)
      IF(ABS(FNLI).GT.0.01) GO TO 10
      SUM = XI*SUM
      IF(I.EQ.25) GO TO 20
   10 SUM = XI*(SUM + 1.0/FNLI)
   20 CONTINUE
      FJN = FN*(SUM - XI**FN*ALOG(XI))
      RETURN
      END



      FUNCTION FJA(A,XI)
      DATA PI/3.1415927/
      SUM = XI/(A + 26.0)
      DO 10 I = 1,25
   10 SUM = XI*(SUM + 1.0/(A + FLOAT(26 - I)))
      ARG = PI*(AMOD(A,1.0) - 0.5)
      FJA = A*(SUM + XI**A*PI*SIN(ARG)/COS(ARG))
      RETURN
      END
```

```
      SUBROUTINE XREFL(THINC,VACLAM,NLAYR,D,DELTA,BETA,RMAG2,NREFL)
      DIMENSION D(20), DELTA(21), BETA(21), CM(2,2), CML(2,2)
      COMPLEX CM, CML, FNCSL, FNCSL1, FNCOS, RL, TL, DL, R
      IF(THINC.NE.0.0) GO TO 10
      RMAG2 = 1.0
      NREFL = NLAYR
      RETURN
   10 CM(1,1) = (1.0,0.0)
      CM(1,2) = (0.0,0.0)
      CM(2,1) = (0.0,0.0)
      CM(2,2) = (1.0,0.0)
      NLR1 = NLAYR + 1
      D(NLR1) = 0.0
      TNET = 1.0
      DO 30 NL = 1,NLR1
      NREFL = NLR1 - NL
      FNCSL1 = CMPLX(THINC,0.0)
      IF(NL.GT.1) CALL SFNCOS(THINC,DELTA(NL-1),BETA(NL-1),FNCSL1)
      CALL SFNCOS(THINC,DELTA(NL),BETA(NL),FNCSL)
      RL = (FNCSL1 - FNCSL)/(FNCSL1 + FNCSL)
      TL = (2.0,0.0)*FNCSL1/(FNCSL1 + FNCSL)
      DL = CMPLX(6.283185*D(NL)/VACLAM,0.0)*FNCSL
      IF(CABS(TL).LT.1.0E-4) GO TO 40
      IF(-AIMAG(DL).GT.9.0) GO TO 40
      TNET = TNET*CABS(TL)*EXP(AIMAG(DL))
      IF(TNET.LT.1.0E-4) GO TO 40
      IF(NL.NE.NLR1) GO TO 20
      IF(REAL(FNCSL)/CABS(FNCSL).GT.1.0E-4) NREFL = -1
      GO TO 30
   20 CML(1,1) = CEXP((0.0,1.0)*DL)/TL
      CML(1,2) = RL*CEXP((0.0,-1.0)*DL)/TL
      CML(2,1) = RL*CEXP((0.0,1.0)*DL)/TL
      CML(2,2) = CEXP((0.0,-1.0)*DL)/TL
      CALL MATMPY(CM,CML,CM)
   30 CONTINUE
   40 R = (CM(2,1) + RL*CM(2,2))/(CM(1,1) + RL*CM(1,2))
      RMAG2 = CABS(R)**2
      RETURN
      END
```

```
      SUBROUTINE SFNCOS(THINC,DELTA,BETA,FNCOS)
      COMPLEX FNCOS
      FTDB = SQRT(0.5*(SQRT((THINC**2 - 2.0*DELTA)**2 + 4.0*BETA**2)
     +  + ABS(THINC**2 - 2.0*DELTA)))
      IF(BETA.NE.0.0) GO TO 10
      FNCOS = CMPLX(FTDB,0.0)
      IF(THINC**2.LT.2.0*DELTA) FNCOS = CMPLX(0.0,-FTDB)
      RETURN
   10 FNCOS = CMPLX(FTDB,-ABS(BETA)/FTDB)
      IF(THINC**2.LT.2.0*DELTA) FNCOS = CMPLX(ABS(BETA)/FTDB,-FTDB)
      RETURN
      END



      SUBROUTINE MATMPY(C1,C2,C12)
      DIMENSION C1(2,2), C2(2,2), C12(2,2), C(2,2)
      COMPLEX C1, C2, C12, C
      DO 10 I=1,2
      DO 10 J=1,2
      C(I,J) = (0.0,0.0)
      DO 10 K=1,2
   10 C(I,J) = C(I,J) + C1(I,K)*C2(K,J)
      DO 20 I=1,2
      DO 20 J=1,2
   20 C12(I,J) = C(I,J)
      RETURN
      END
```

```
      SUBROUTINE GOPLT(PRID,FACT)
      XTOT = 510.0
      YTOT = 11.0
      CALL PLOID3(PRID,XTOT,YTOT,FACT)
      CALL PLOT(9.75,.5,3)
      CALL PLOT(9.75,.7,2)
      CALL PLOT(9.75,7.8,3)
      CALL PLOT(9.75,8.0,2)
      CALL PLOT(9.95,8.0,2)
      CALL PLOT(9.55,8.0,2)
      CALL PLOT(0.0,.5,-3)
      RETURN
      END



      SUBROUTINE CRVPLT(X,Y,N,BCD,ICIRC)
      COMMON/PLTR/XMAXC,XMINC,YMAXC,YMINC,DX,DY,XINCH,YINCH
      DIMENSION X(300),Y(300)
      DIMENSION XMOD(300),YMOD(300)
      IC = 0
      IF(ICIRC .NE. 0)  IC = 1
      II = 0
      DO 10 I = 1, N
      IF(XMINC .LE. X(I) .AND. X(I) .LE. XMAXC)II = II + 1
      IF (XMINC .LE. X(I) .AND. X(I) .LE. XMAXC) XMOD(II) = X(I)
      IF (XMINC .LE. X(I) .AND. X(I) .LE. XMAXC)  YMOD(II) = Y(I)
   10 CONTINUE
      IF(II .EQ. 0)  RETURN
      DO 20 I = 1, II
      IF (YMOD(I) .LT. YMINC) YMOD(I) = YMINC
      IF (YMOD(I) .GT. YMAXC)  YMOD(I) = YMAXC
   20 CONTINUE
      CALL LINE(XMOD,YMOD,II,1,IC,1,XMINC,DX,YMINC,DY,.08)
      XWHERE = (XMOD(II)-XMINC)*XINCH/(XMAXC-XMINC) + .1
      YWHERE = (YMOD(II)-YMINC)*YINCH/(YMAXC-YMINC) -.05
      CALL SYMBOL(XWHERE,YWHERE,.1,BCD,0.0,1)
      RETURN
      END
```

```
      SUBROUTINE FRMPLT(XMIN,XMAX,NYCALC,YMIN,YMAX,X,Y,N)
      COMMON/PLTR/XMAXC,XMINC,YMAXC,YMINC,DX,DY,XINCH,YINCH
      DIMENSION X(300),Y(300)
      DATA XINCH/9.0/,YINCH/7.0/
      CALL PLOT(11.0,0.0,-3)
      IF(NYCALC .EQ. 0)  GO TO 20
      YMAX = Y(1)
      YMIN = Y(1)
      DO 10 I = 1, N
      IF (X(I) .LT. XMIN .OR. X(I) .GT. XMAX)  GO TO 10
      IF (Y(I) .LE. YMIN)  YMIN = Y(I)
      IF (Y(I) .GE. YMAX)  YMAX = Y(I)
   10 CONTINUE
   20 IF (XMAX .LE. XMIN)  RETURN
      DX = ABS(XMAX - XMIN)/10.0
      IF(ALOG10(DX) .LT. 0.0) NMINX=IFIX(ALOG10(DX))-1
      IF(ALOG10(DX) .LT. 0.0)  GO TO 30
      NMINX = ALOG10(DX)
   30 CONTINUE
      DXRD = DX*10.0**(-NMINX)
      IF (DXRD .GE. 1.0)  DX = 1.0
      IF (DXRD .GE. 2.0)  DX = 2.0
      IF (DXRD .GE. 2.5)  DX = 2.5
      IF (DXRD .GE. 5.0)  DX = 5.0
      DX = DX*10.0**NMINX
      XMNFRM = FLOAT(IFIX(XMIN*1.0001/DX))*DX
      IF (XMIN .LT. 0.0)  XMNFRM = XMNFRM - DX
      XMXFRM = FLOAT(IFIX(XMAX*0.9999/DX) )*DX
      IF (XMAX .GT. 0.0)  XMXFRM = XMXFRM + DX
      IF (YMAX .LE. YMIN)  RETURN
      DY = ABS(YMAX - YMIN)/10.0
      IF(ALOG10(DY) .LT. 0.0) NMINY = IFIX(ALOG10(DY))-1
      IF(ALOG10(DY) .LT. 0.0)  GO TO 40
      NMINY = ALOG10(DY)
   40 CONTINUE
      DYRD = DY*10.0**(-NMINY)
      IF (DYRD .GE. 1.0)  DY = 1.0
      IF(DYRD .GE. 2.0)  DY = 2.0
      IF(DYRD .GE. 2.5)  DY = 2.5
      IF (DYRD .GE. 5.0)  DY = 5.0
      DY = DY*10.0**NMINY
      YMNFRM = FLOAT(IFIX(YMIN*1.0001/DY))*DY
      IF (YMIN .LT. 0.0)  YMNFRM = YMNFRM - DY
      YMXFRM = FLOAT(IFIX(YMAX*0.9999/DY))*DY
      IF (YMAX .GT. 0.0)  YMXFRM = YMXFRM + DY
      XMINC = XMNFRM
      XMAXC = XMXFRM
      YMINC = YMNFRM
      YMAXC = YMXFRM
      DVX = (XMAXC - XMINC)*10.0/(DX*XINCH)
      DVY = (YMAXC - YMINC)*10.0/(DY*YINCH)
      DX = (XMAXC - XMINC)/XINCH
      DY = (YMAXC - YMINC)/YINCH
```

```
      CALL AXIS (0.0,0.0,21HINC. ANGLE (ARC MIN.),-21,XINCH,0.0,XMINC,
     +    DX,DVX)
      CALL AXIS (0.0,0.0,11HREFLECTANCE,11,YINCH,90.0,YMINC,DY,DVY)
      CALL PLOT( 0.0,YINCH,3)
      CALL PLOT(XINCH,YINCH,2)
      CALL PLOT(XINCH,0.0,2)
      IF(XMAXC*XMINC .GE. 0.0)  GO TO 80
      XZERO = -XMINC*XINCH/(XMAXC-XMINC)
      CALL PLOT (XZERO,0.0,3)
      CALL PLOT (XZERO,YINCH,2)
   80 CONTINUE
      IF (YMAXC*YMINC .GE. 0.0)  GO TO 90
      YZERO = -YMINC*YINCH/(YMAXC-YMINC)
      CALL PLOT ( 0.0,YZERO,3)
      CALL PLOT(XINCH,YZERO,2)
   90 CONTINUE
      XTEAR = XINCH + .75
      XTEAR1 = XINCH + .95
      XTEAR2 = XINCH + .55
      YTEAR = YINCH + .3
      YTEAR1 = YINCH + .5
      CALL PLOT(XTEAR,0.0,3)
      CALL PLOT(XTEAR,.2,2)
      CALL PLOT(XTEAR,YTEAR,3)
      CALL PLOT(XTEAR,YTEAR1,2)
      CALL PLOT(XTEAR1,YTEAR1,2)
      CALL PLOT(XTEAR2,YTEAR1,2)
      RETURN
      END
```

REFERENCES

1. J. D. Jackson, Classical Electrodynamics, John Wiley and Sons, Inc., New York, 1965.

2. J. A. Stratton, Electromagnetic Theory, Mc-Graw-Hill Book Co., Inc., New York, 1941.

3. M. V. Klein, Optics, John Wiley and Sons, Inc., New York, 1970.

4. O. S. Heavens, Reports on Progress in Physics, 23, 1 (1960).

5. A. H. Compton and S. K. Allison, X-Rays in Theory and Experiment, D. vanNostrand Co., Inc., New York, 1935.

6. L. D. Landau and E. M. Lifschitz, Electrodynamics of Continuous Media, Addison-Wesley Publishing Co., Inc., Massachusetts, 1960.

7. L. G. Parratt and C. F. Hempstead, Phys. Rev. 94, 1593, (1954).

8. H. A. Kramers, Nature 114, 310, (1929)

9. H. vonKallmann and H. Mark, Ann. Physik Ser IV, 82, 585, (1927)

10. R. D. Evans, The Atomic Nucleus, McGraw-Hill Book Co., Inc., New York, 1955.

11. L. G. Parratt, Phys. Rev. 95, 359, (1954).